Naval Surface Warfare Center
Carderock Division
West Bethesda, MD 20817-5700

NSWCCD-61-TR–2007/02 July 2008

Survivability, Structures and Materials Department

Technical Report

Mechanism of Corrosion Product Growth on Nickel Aluminum Bronze/10% Ammonia – 90% Seawater Interface: Effect of Applied External Stress

by

A. Srinivasa Rao

NSWCCD-61-TR–2007/02 Mechanism of Corrosion Product Growth on Nickel Aluminum Bronze/10% Ammonia – 90% Seawater Interface: Effect of Applied External Stress

Naval Surface Warfare Center
Carderock Division
West Bethesda, MD 20817-5700

NSWCCD-61-TR–2007/02 July 2008

Survivability, Structures and Materials Department

Technical Report

Mechanism of Corrosion Product Growth on Nickel Aluminum Bronze/10% Ammonia – 90% Seawater Interface: Effect of Applied External Stress

by

A. Srinivasa Rao

This page intentionally left blank

REPORT DOCUMENTATION PAGE

Form Approved
OMB No. 0704-0188

1. REPORT DATE *(DD-MM-YYYY)*	**2. REPORT TYPE**	**3. DATES COVERED** *(From - To)*
July 2008	Research and Development	

4. TITLE AND SUBTITLE

Mechanism of Corrosion Product Growth on Nickel Aluminum Bronze /10% Ammonia – 90% Seawater Interface: Effect of Applied External Stress

5a. CONTRACT NUMBER

5b. GRANT NUMBER

5c. PROGRAM ELEMENT NUMBER

6. AUTHOR(S)

A. Srinivasa Rao

5d. PROJECT NUMBER

5e. TASK NUMBER

5f. WORK UNIT NUMBER

7. PERFORMING ORGANIZATION NAME(S) AND ADDRESS(ES) AND ADDRESS(ES)

NAVAL SURFACE WARFARE CENTER
CARDEROCK DIVISION (CODE 612)
9500 MACARTHUR BLVD
WEST BETHESDA MD 20817-5700

8. PERFORMING ORGANIZATION REPORT NUMBER

NSWCCD 61-TR-2007/02

9. SPONSORING / MONITORING AGENCY NAME(S) AND ADDRESS(ES)

NAVAL SURFACE WARFARE CENTER
CARDEROCK DIVISION (CODE 612)
9500 MACARTHUR BLVD
WEST BETHESDA MD 20817-5700

10. SPONSOR/MONITOR'S ACRONYM(S)

11. SPONSOR/MONITOR'S REPORT NUMBER(S)

12. DISTRIBUTION / AVAILABILITY STATEMENT

Distribution unlimited. Approved for public release

13. SUPPLEMENTARY NOTES

14. ABSTRACT

This investigation was undertaken to develop a corrosion process model based on the chemical reaction kinetics in materials. A mathematical model relating the process parameter (viz. the weight change, the measured open circuit potentials (versus SCE) and the change in the structure of the material) and the reaction time was developed. This model was tested with nickel aluminum bronze (NAB) samples in 10% NH_4OH – 90% seawater solution, and the kinetics parameters such as the rate constant and the order of reaction, were determined. In addition, the effect of applied external stress on the corrosion process was also investigated.

The nickel aluminum bronze (NAB) samples were exposed to 10% NH4OH -90% seawater solution for up to 46 days. In addition, some samples were subjected to the continuous application of 7.5 ksi and 15 ksi stress. The weight change was measured on all samples. Similarly the structure of the corroded sample surface was determined from their x-ray diffraction patterns. The weight change data and the structural analysis based information were fed into the reaction kinetics model and the oxide characteristics were determined. Results suggest that the kinetic parameter such as the order of reaction for the corrosion process that was predicted by (over)

over15. SUBJECT TERMS

Nickel Aluminum Bronze; Ammonia; Seawater; Reaction Kinetic

16. SECURITY CLASSIFICATION OF:			**17. LIMITATION OF ABSTRACT**	**18. NUMBER OF PAGES**	**19a. NAME OF RESPONSIBLE PERSON**
a. REPORT	**b. ABSTRACT**	**c. THIS PAGE**			A. Srinivasa Rao
UNCLASSIFIED	**UNCLASSIFIED**	**UNCLASSIFIED**	**SAR**	**62**	**19b. TELEPHONE NUMBER** *(include area code)* 301-227-5141

14. ABSTRACT (Continued)

feeding all three sets of data into the model indicates that the corrosion of NAB in 10% NH4OH - 90% seawater is a diffusion controlled process. The kinetics of the fast reaction stage is controlled by the availability of NAB sample surface for corrosion. The slow chemical reaction stage is very complex. The complexity is perhaps due to the nucleation and growth of complex and mixed oxides/hydroxides. During the corrosion process the rate of corrosion of iron is the highest and the corrosion of the nickel is the slowest. The rate of corrosion increases with an increase in the applied stress.

Contents

This page intentionally left blank

Figures (Cont.)

Figures (Cont.)

Figures (Cont.)

Tables

Administrative Information

The work described in this report was performed at the Naval Surface Warfare Center, Carderock Division (NSWCCD), West Bethesda, MD. in the Survivability, Structures and Materials Department (Code 60) by the Materials Division (Code 61). The project was funded from the Code 61 Internal Overhead Funds.

Acknowledgements

The author would like to thank Dr. Catherine Wong and Ms. Angela Felker (Code 612) for their technical discussions and scanning electron micrograph of the NAB samples after corrosion and for proof reading and correcting the manuscript. The author also acknowledges the use of the x-ray diffraction facilities purchased by the Geology Department of the George Washington University, Washington D.C.

This page intentionally left blank

EXECUTIVE SUMMARY

In order to develop a model of the corrosion process based on the chemical reaction kinetics in materials, this investigation was undertaken. A mathematical model relating the process parameter (viz. the weight change, the measured open circuit potentials (versus SCE) and the change in the structure of the material) and the reaction time was developed. This model was tested with nickel aluminum bronze samples in 10% NH_4OH – 90% seawater solution, and the kinetics parameters such as the rate constant and the order of reaction, were determined. In addition, the effect of applied external stress on the corrosion process was also investigated.

The nickel aluminum bronze (NAB) samples were exposed to 10% NH_4OH - 90% seawater solution for up to 46 days. In addition, some samples were subjected to the continuous application of 7.5 ksi and 15 ksi stress. The weight change was measured on all samples. Similarly, the structure of the corroded sample surface was determined from their x-ray diffraction patterns. The weight change data and the structural analysis based information were fed into the reaction kinetics model and the oxide characteristics were determined. The results suggest that the kinetic parameter such as the order of reaction for the corrosion process indicates that the corrosion of NAB in 10% NH_4OH - 90% seawater is a diffusion controlled process. The kinetics of the fast reaction stage is controlled by the availability of NAB sample surface for corrosion. The slow chemical reaction stage is very complex. The complexity is perhaps due to the nucleation and growth of complex and mixed oxides/hydroxides. During the corrosion process the rate of corrosion of iron is the highest and the corrosion of the nickel is the slowest. The rate of corrosion increases with an increase in the applied stress.

INTRODUCTION

Process modeling is an efficient method to understand a specific process and optimize the process variables. Modeling requires first training a sequence of logical realities and then deriving proper conclusions as dependable mathematical relationships. For example, during simple corrosion of a metal, although one observes the formation of an oxide layer on the metal surface, several other properties such the potential, structure and mechanical strength also change. Since these properties are related to the chemistry and physics of the metal, it is possible to correlate all the inter-related properties. In order to ascertain some fundamental relationships

between the rate of corrosion and the order of the chemical reaction and the nature of the oxide film, the experimental database was obtained from systematic corrosion studies.

The aim of the present investigation is to study the corrosion kinetics of nickel aluminum bronze in 10% ammonia and 90% seawater solution with and without the concurrent application of applied external stress and model the process. The purpose of the present investigation is to test whether the developed kinetics process model can predict the growth and morphology of corrosion products.

Theory

In general, it can be hypothesized that as the electrochemical reaction progresses, the reaction products continue to grow. While the change in the metal surface concentration that is actively taking part in the electrochemical process has a finite functionality (i.e. the concentration changes with time), the concentration of the corroding media remains constant (the solution concentration remains unchanged or the change in the concentration ratio between the metal and solution is negligible). If two active species are continuously changing to form the products, the rate of change of the concentration can be represented as follows [1]:

$$\mathbf{(dx/dt) = k\,(a-x)\,(b-x)\ or}$$

$$\mathbf{k = (1/\{t(a-b)\})\ ln\ [\{a - (a-b)\}\{(a-x)\}/\{(a)\ ((a-x)-(a-b))\}]} \qquad \mathbf{[1]}$$

where ‘k’ is the rate constant and ‘a’ and ‘b’ are the initial concentrations of the *two species* and ‘x’ is the concentration of ‘a’ or ‘b’ at after *time* ‘t’. Similarly, if the number of components that are changing with time are ‘n’, the rate of change is given as

$$\mathbf{(dx/dt) = k\,(a-x)n\quad or}$$

$$\mathbf{n = [\{ln\ (-dx1/dt) - ln\ (-dx2/dt)\}/\{(log\ (x1)) - (\ log\ (x2)\ )\}]} \qquad \mathbf{[2]}$$

where ‘(dx_1/dt)’, ‘(dx_2/dt)’ are the rate of change of concentration at ‘(x_1)’, ‘(x_2)’ respectively.

The above expression for the overall buildup of all oxides due to corrosion can be rewritten in terms of rate of change of weight with time as

$$\mathbf{(dw/dt) \propto\ -\{(dwoxide/dt)\ or}$$

$$\mathbf{(dw/dt) =\quad A\ \{\ (dwoxide/dt)} \qquad \mathbf{[3]}$$

where A is a constant.

The overall oxide formation depends upon the reaction kinetics and it will be fast at the beginning and very slow at the end. Generally the slow reaction stage is preceded with an intermediate reaction zone. The overall oxide formation during any one of the stages could depend upon several parameters such as direct chemical reaction with the metal surface, a reaction process that involves the diffusion of reacting liquid to reach the new metal surface, a reverse kinetics due to the reduction of formed metal oxide to the metal etc. All the above chemical processes influence the chemical reaction at any given time. Figure 1 shows a schematic diagram of an oxide buildup versus time plots that can be noted during a typical electrochemical reaction.

From Figure 1, it can be understood that the electrochemical process initially occurs at a faster rate (i.e. Stage I). Next the kinetics proceeds at a slower rate (Stage II), and eventually the reaction precede at a much slower pace (Stage III) or sometimes, the reaction shows a trend that the reverse process is taking place.

During Stage I, the corrosion / electrochemical reaction proceeds at a faster rate as a result of unimpeded chemical reaction between metal and the corroding medium. Therefore, it can be assumed that during Stage I,

The overall chemical reaction rate at

Stage I (Fast oxide growth stage) $\left((dw/dt)_{\text{Stage I}}\right) = A(w_1 / t_1)$ **[4]**

The Stage II reaction represents a transitional zone between the fast and slow chemical reaction (i.e. a chemical zone in which a fast reaction process (i.e. first stage) begins to slow down and the oxide build up begins at a slower pace). In many reactions, the transitional zone may be small, so that this region can be ignored. However, for the process in which diffusion is important, the overall rate of reaction in Stage II is given as

Stage II (Intermediate stage) $(dw/dt)_{\text{Stage II}} = A\,(w2-w1) / (t2-t1)$ **[5]**

During Stage III, a slow and steady chemical reaction continues with time and a continuous build up of a third oxide at a slower reaction rate can be seen. Therefore, the overall rate of reaction in Stage III is given as

Stage III (Slow oxide buildup stage) $(dw/dt)_{\text{Stage III}} = A\,(w_3 - w_2) / (t_3 - t_2)$ **[6]**

In metallurgical processes such as the oxidation and reduction of metal alloys, the oxide growth imparts a steady effect on the electrical, mechanical, and or structural properties of the host metal. If the growth of oxide is uniform, the information (viz. electrical, mechanical and structural properties) obtained on the oxidized metal can be assumed to follow the kinetics of the oxidation process. For example, the rate of oxidation can be treated in terms of the normalized change in the structure or change in the mechanical properties or the electrical properties. Thus, the above relationships obtained for different stages can be rewritten as follows:

The overall rate of chemical reaction ≈ rate of change in the structure of material at Stage I

$$\textbf{Stage I (Fast oxide growth stage)} \quad (dS/dt)_{\text{Stage I}} = B\,(S_1 / t_1) \qquad [7]$$

where B is a constant, and 'S' represents the normalized volume fraction and /or the area fraction of a newly formed structure as result of chemical reaction at time 't'.

The Stage II reaction represents a transition zone between the fast and slow chemical reaction (i.e. a chemical zone in which a fast reaction process (i.e. first stage) begins to slow down and the oxide buildup begins at a slower pace). It has to be emphasized that in many reactions, the transitional zone may be small, so that this region can be ignored.

The overall rate of reaction in Stage II is given as

$$\textbf{Stage II (Intermediate stage)} \quad (dS/dt)_{\text{Stage II}} = B\,(S_2 - S_1) / (t_2 - t_1) \qquad [8]$$

During the third stage, a slow and steady chemical reaction continues with time and a continuous change in the structure of the host occurring at a slower reaction rate can be seen.

Therefore, the overall rate of reaction in Stage III is given as

Stage III (Slow oxide buildup stage)

$$(dS/dt)_{\text{Stage III}} = B\,(S_3 - S_2) / (t_3 - t_2) \qquad [9]$$

The above equations provide solutions for the rate of the oxide film growth and the magnitude of the film growth represents the severity of the corrosion. However, the rate parameter will not provide a detailed analysis of the type of the chemical reaction (viz. the number of components that are participating in the corrosion process, the nature of chemical reaction etc.).

The general characteristics of oxide that is formed at a faster rate will have oxide that is irregular, coarse, non-uniform, and loose and have a porous morphology. The oxide that is

dominated by the diffusion process will have a porous morphology while the oxide that forms slowly will have a dense and uniform microstructure. The oxide formed as a result of fast reaction kinetics and the diffusion will have severe oxide cracking similar to that of mud cracking while the oxide that formed slowly with a slow diffusion of liquid will have uniform oxide with fine pores.

In order to understand the chemistry of the process, the original reaction kinetics equation, Equation 1 can be rewritten in terms of fast oxide growth, diffusion controlled oxide growth, and slow oxide growth as follows:

$$(dw_{oxide}/dt) = (dw_{fast\ oxide\ growth}/dt) + (dw_{diffusion}/dt) + (dw_{slow\ oxide\ growth}/dt) \quad [10]$$

During the chemical reaction, if the oxide is assumed to form primarily due to fast chemical reaction between the metal and the corroding liquid, and the time required for the diffusion of the liquid to find new metal surface is small, then the rate of oxide build due to diffusion and the rate of other processes can be ignored. Therefore the overall corrosion process can be rewritten as:

$$(dw_{oxide}/dt) = (dw_{fast\ oxide\ growth}/dt) \quad [11]$$

Similarly, if the oxide formation requires the diffusion of solution (through the pores of oxide formed) to find new metal surface, then the rates of other processes can be ignored. Therefore the overall corrosion process can be represented as:

$$(dw_{oxide}/dt) = (dw_{diffusion}/dt) \quad [12]$$

If the oxide formation requires long chemical reaction time and the rate determining step is only the slow chemical reaction, the other faster chemical processes (viz. diffusion etc.) can be ignored. Therefore during this process, the overall corrosion process is given as:

$$(dw_{oxide}/dt) = (dw_{slow\ oxide\ growth}/dt) \quad [13]$$

If it is assumed that the corroding liquid concentration remains constant and only the concentration of the metal species change with time, the integrated form of the corrosion process kinetic rate equations are given in terms of concentration (c) of the reacting species as:

$$\ln\{(dc_1/dt_1) / (dc_2/dt_2)\} = -n\{\ln(c_1) - \ln(c_2)\} \quad [14]$$

$$\text{or} \quad n = -[\ln\{(dc_1/dt_1) / (dc_2/dt_2)\} / \{\ln(c_1) - \ln(c_2)\}] \quad [15]$$

where 'n' is the order of reaction, and 'c_1' and 'c_2'are the concentration of the reactants at time 't_1' and 't_2' and (dc_1/dt_1) and (dc_2/dt_2) are the slopes measured by drawing a tangent to the concentration versus time curves at ((t_1, c_1) and (t_2, c_2)} respectively. The above equation represents typical transformation of the functionality of the generalized equation [Equation 2]. The value of 'n' equals to 'one' means that the concentration of 'one species' is continuously changing with time while the value of n equals to *two* means that the concentration of two species are changing continuously. The value of 0.5 and 0 represents the chemical reaction that is controlled by the diffusion process and time dependent process respectively. A mixed value of 1.5 represents a chemical reaction in which the concentration of one species is changing continuously with the reaction time. In addition, the diffusion process also influences the chemical reaction.

EXPERIMENTAL PROCEDURE

Materials and Testing

During the present investigation two different sets of experiments were conducted and the results were used to model the corrosion process. The experimental measurements were the determination of weight change, and the change in the structure of the material during corrosion of nickel aluminum bronze (NAB) in ammonia or seawater.

The weight change measurements were made by measuring the weight of NAB samples both before and after the corrosion. The samples were weighed and were inserted into the beaker containing 10% ammonia – 90% seawater. The NAB samples were removed from the solution and quickly dried in a vacuum desiccator. The samples were weighed and the change in the weight of the NAB sample due to corrosion was determined. From the weight change, the normalized weight change was calculated.

In the second set of experiments, the NAB samples were cut to form rectangular samples of 50 mm length, 5 mm width and 1 mm thickness. The samples were polished to a 1micron diamond finish. The samples were positioned in a specially built three-point bend test assembly that was designed and built for the stress corrosion testing.

The change in the structure of the nickel aluminum bronze was measured using x-ray diffraction method. A Sintag XDS-2000 x-ray diffractometer with a $CuK_{\alpha 1}$ source at 8048 eV, -2.5 FWHM was used during this investigation. The x-ray energy and the current were 35 KV,

and 30 mA, respectively. The NAB samples were subjected to corrosion in ammonia solution or seawater. The samples were removed and quickly dried in a vacuum desiccator. The samples were mounted on the x-ray diffraction unit and the structure was recorded as a function of the angle of incidence (2θ).

During the present analysis reagent grade ammonia solution and simulated seawater were used as the corrosion media. The simulated seawater was prepared using the ASTM standard procedure. The concentration of the solution is 10% ammonia and 90% simulated seawater. For convenience, the solution was labeled as 10% ammonia – 90% seawater. All the experiments were conducted for about 45 days.

Stress Corrosion Test Cell

The stress corrosion test cell (SCTC) was a three point bend test unit. It was fabricated using a rectangular 70 mm X 50 mm X 25 mm Teflon block. The schematic diagram of the SCTC is given in Figure 2. The test cell positions a thin test bar on two roller bearings. The stress was applied at the center of the freely suspended beam. In order to prevent the slipping of the suspended beam during the entire corrosion study, a safe sample guarding mechanism was incorporated on the SCTC. A predetermined weight provided the required stress on the sample. During the present study, a constant stress of either 7.5 ksi or 15 ksi was applied to the NAB samples.

Figures 3 – 5 shows the SCTC used during this investigation. From Figures 3-5, the positioning of the NAB test samples, the applied load, the 10% ammonia-90% seawater liquid level and the corrosion products formed on the NAB sample surface can be observed clearly.

RESULTS AND DISCUSSION

Figure 6 shows the normalized weight change versus corrosion time for nickel aluminum bronze (NAB) in 10% NH_4OH –90% seawater subjected to the continuous application of external stress 0, 7.5 and 15 ksi respectively.

The results suggest that the chemical reaction between NAB and 10% NH_4OH and 90% seawater has two distinctive chemical reaction zones or stages [ie. ((i). fast oxide growth stage and (ii). slow oxide buildup stage)]. From the above figures, qualitatively, it can be suggested that the (%) weight change for NAB in 10% NH_4OH and 90% seawater is higher under applied external stress than normal corrosion of NAB in 10% NH_4OH and 90% seawater. The rate of the reaction and the order of reaction for the overall process were determined by drawing tangents for the normalized weight change versus reaction time plots at two concentrations and determining the slopes at those two concentrations. Similarly, the order of reaction for a given stage was determined by taking the slope at two concentrations within the limits of that stage.

The overall rate of the reaction, the rate of fast (first stage) reaction and the slow (second stage) reaction process and their corresponding order of the reactions are given Table 1. The results shown in Table 1 show that NAB sample under 15 ksi stress lost more than 3 times the amount of material lost per day than the amount of material lost under normal stress free condition. The order of the reaction results suggest that the overall corrosion of NAB in 10% NH_4OH – 90% seawater is primarily a diffusion controlled process. The slow oxide build up stage is a process that involves complex chemical reaction in which several reactants are actively participating.

The Figures 7-14; 16-23 and 25-32 represent the x-ray diffraction data obtained from nickel aluminum bronze (NAB) samples reacted with 10% NH4OH solution and 90 % seawater with 7.5 ksi stress (Figures 16-23), 15 ksi stress (Figures 25-32) and without the concurrent application of external stress (Figures 7-14). The results shown in the figures suggest that the peaks for NAB in 10% NH_4OH solution and 90% seawater are distinct and well defined.

In order to quantify the ratio between the reactants and products, the x-ray data was reanalyzed as follows: First, the information on the standard peaks for all elements in the NAB and their corresponding oxides and hydroxides was collected. By carefully analyzing the

information, a specific "2 theta" angle was selected for each element / compound. A standard chart was prepared. The standard peaks were then noted in all the x-ray diffraction patterns. Second, the area under those peaks was measured. The oxide/hydroxide formed during the corrosion process was obtained by adding the total areas of all metal oxides and the metal hydroxides. The fraction of oxides/hydroxides formed at a given time is determined by dividing the total oxides/hydroxides formed by the sum of the areas of both oxides/hydroxides and the metal species. Similarly, the amount of a specific oxide/hydroxide (viz. copper oxide/hydroxide) formed during corrosion was determined by dividing the total value of the copper oxides/hydroxides by the sum of the total oxides/hydroxides plus the total area under the copper peak. The estimated oxides/hydroxides based on the x-ray structural determination were plotted as a function of corrosion time.

Figures 15, 24 and 33 show the comparative plots of the oxides/hydroxides formed on the surface of NAB due to chemical reaction with 10% NH_4OH solution and 90% seawater. The results shown in Figures 15, 24 and 33 corresponds to the corrosion experiments conducted under 0, 7.5 and 15 ksi stress levels respectively. The results suggest that the oxides/hydroxide buildup on the surface constitutes two distinctive phases. That is the fast oxide growth followed by a slow oxide buildup.

Using the chemical reaction kinetic equations (5-7), the data from the oxides/hydroxides that formed on the surface was analyzed. The rate of the reaction and the order of reaction for the overall process, fast reaction phase and slow reaction phase were determined and the results are given in Tables 2-4 respectively. The results suggest that the overall reaction process is close to that of the corrosion process of copper. That is, the formation of copper oxides/hydroxides determines the overall corrosion process of NAB. The results also suggest that while corrosion kinetics of nickel in NAB is the slowest, the degradation of iron is the highest of the alloying elements.

From the structural analysis data, it is clear that the corrosion rate of nickel aluminum bronze in 10% NH_4OH and 90% seawater varies for different metallic species. This is due to the difference in the rate of corrosion of the metallic components of the alloy.

The important result that is discernible from the structure-based analysis is the higher rate of removal of copper from the NAB sample followed by iron, aluminum, and nickel. While copper is the major constituent of the NAB, it is surprising to notice that at any given time, most

of the oxide/hydroxide formation comes from iron. Iron is present in NAB as a fine precipitate with the aluminum. The iron aluminide forms a phase known as kappa (II) phase and it is distributed throughout the NAB matrix. In addition, aluminum also forms an inter-metallic nickel aluminide (Kappa (III) phase) and it is also equally distributed throughout the NAB sample. Since the rate of removal of nickel is the lowest in the overall reaction, it is reasonable to suggest that the aluminum oxide/hydroxide formed during corrosion process comes from the aluminum that is held with iron or aluminum in solution in the copper matrix.

If one assumes that the total aluminum depleted from NAB is from iron aluminide, the weight loss due to corrosion can be hypothesized in two ways. (1) The iron and aluminum in NAB continuously reacts with the corrosion medium (i.e.NH_4OH or seawater) and form their corresponding oxides/hydroxides on the sample surface; or (2) the matrix that surround the kappa (II) phase is continuously being reacted by the corroding liquid. As a result the adhesion and bonding of embedded kappa (II) phase (Fe_3Al) with the matrix (NAB) is lost. The net result is the removal of kappa (II) phase particles. Figure 34 shows a schematic diagram of how an embedded kappa phase particle can be removed as a result of the dissolution of the surrounding matrix phase.

If it is assumed that the formation and growth of iron and aluminum oxides/hydroxides is only due to the chemical reaction between kappa (II) phase and the corroding solution, the total sample surface must be covered with iron and aluminum oxides/hydroxides. However, the structural analysis indicates that the surface is also covered with significant amounts of copper and some nickel oxides/hydroxides. If one attributes the removal of kappa phase via the second mechanism, one would not expect to see the presence of large amounts of iron or aluminum oxides/hydroxides on the sample surface. It is possible that the removal of kappa (II) phase constitutes both the dissolution of some iron aluminide to form iron and aluminum oxides/hydroxides (mechanism 1) and the removal due to the removal of matrix phase around the kappa particles (mechanism 2). If such complex processes are occurring in NAB/10% NH_4OH-90% seawater systems, the degradation of the NAB should accelerate with the concurrent and continuous application of stress (Figure 34).

The present results that were obtained from weight change method and x-ray structure based analysis validate the above hypothesis. In addition, the present results also show a surprising anomaly. That is, even at zero time, the amount of oxides on the surface is significant

(Tables 2-4). At the present, we have no validated explanation for this anomaly. However, in order to understand and explain the reason for such significant oxide presence on the surface, we are addressing this problem from a number of directions. One theoretical approach is to generate the reaction kinetics plots for the corrosion process based on classical chemistry of solid – liquid interfaces and try to determine whether the reaction kinetics based models can explain our observations. The second approach is to determine the amount of passive oxide film on the surface of as received NAB and try to explain the observed anomaly.

It has been suggested that chemical reactions of order "n" can take place by rate controlling heterogeneous processes [3,4]. Most of the chemical kinetic reaction processes that involve diffusion and n^{th} order models are limited to solid-state reaction processes [5]. However, these models can be extended to explain the chemistry of solid – liquid interfaces. The experimental limitation is that it is very difficult to make a precise 3-D measurements on the changes in the materials property that are taking place as a function of time. If one assumes that the chemical reaction process is a homogeneous and uniform, the kinetics of the reaction that are controlled by 2- dimensional diffusion and 3- dimensional processes are given as

$$\mathbf{[\{(1-\alpha)\,(\ln(1-\alpha)\}+\alpha] = k\,t} \qquad \mathbf{[16]}$$

and

$$\mathbf{[\,1 - (1-\alpha)^{1/3}]^2 = k\,t} \qquad \mathbf{[17]}$$

where "α" is the volume fraction of the un reacted materials

"**k**" is the chemical reaction rate constant

and "**t**" is the reaction time.

The amount of copper, nickel, aluminum and iron oxide / hydroxide present on the surface of corroded nickel aluminum bronze surface as a function of the corrosion time are shown in Figures 35-38 respectively. The theoretical volume fraction of the oxide/hydroxide versus time that determined using the 2-D and 3-D diffusion kinetics models are also shown in Figures 35-38. The results suggest that the experimental projections are much higher than the predictions based on the diffusion kinetics model. However, the theory based on 2 – dimensional diffusion kinetics appears to agree with the measured data for copper and iron oxide/hydroxides. The important point that has to be recognized is that in all cases analyzed here the actual value is shifted by a constant value.

Careful examination of the experimental kinetic data (Figures 15, 24 and 33) reveals that at time (t) is equal to zero, the amount of oxide/hydroxide on NAB surface was never zero. It was surprising that this value corresponds to the actual shift in the experimental analysis based curve to the theoretical curve predicted using the 2- dimensional diffusion kinetics (Figures 39 and 40). The actual values for the amount of (%) oxide/hydroxide on the surface for zero time are given in Tables 2-4. For convenience, in the tables those values were labeled as (%) correction. If one assumes that the (%) oxide/hydroxide at time zero corresponds to surface oxide, a thorough chemical analysis of the surface and/or the examination of morphology of the surface cross-section using scanning electron microscopy must validate the above assumption. The present results from Table 2 indicate that the NAB samples subjected to corrosion without any external stress are associated with some oxide/hydroxide.

Figures 41 and 42 show typical microstructure of the nickel aluminum bronze viewed through the sample cross-section. Figure 41 is obtained from NAB sample at the start of the corrosion experiment (t=0) while the Figure 42 represents the microstructure of corroded NAB sample. The results suggest that both the NAB samples are associated with considerable amount of oxide surface. However, the oxide surface from the as received NAB does not contain any observable kappa (II) phase (iron aluminide phase) (Figure 41). It is therefore possible that the amount of air oxide on NAB sample surface corresponds to the (%) oxide /hydroxide that were noted in Figure 23 and Table 2. Similarly, the presence of significant number kappa particles embedded in oxide film after 42 days (Figure 42) also explains the faster rate of removal of iron and aluminum /oxides or hydroxides from the corroding surface of NAB. However, the present results shown in Tables 2-4 cannot explain why the concurrent application of external stress increases the (%) oxide/hydroxide on the NAB surface.

The initial oxide/hydroxide (at t=0) also increases with an increase in the external stress. If the oxide/hydroxide is only the air oxide film, the external stress application should not increase the amount of oxide/hydroxides on the surface. This concludes that the mechanism of the corrosion of NAB under stress is different. A second possible mechanism can be suggested as follows: Initially the NAB is associated with air oxide. For the corrosion of NAB to continue the surface oxide layer must be broken. It is only when the surface oxide film is broken, the corroding media (i.e. the ammonia – saltwater solution) can come into contact with the bare metal/alloy and react chemically. Such process may require the application of some external

stress. It is possible that the measured increase in the initial (%) oxide/hydroxide values in (Tables 3 and 4) is related to the applied external stress. At present qualitatively, it can be speculated that the application of external stress produces cracks in the oxide film and the corrosion starts. As the first layer of the NAB matrix is corroded, the external stress forces the dispersed kappa (II) phase to also leave the matrix and become a part of the oxide layer. In order to unequivocally prove the present hypothesis, a thorough and complete microstructural examination is being carried out using scanning electron microscopy.

CONCLUSIONS

From the present analysis the following conclusions can be made:

1. The kinetics of the corrosion process of nickel aluminum bronze (NAB) in 10% NH_4OH-90% seawater that was determined using weight change measurements, and structure change analysis suggest that the overall kinetic process is diffusion controlled.
2. The corrosion of NAB in ammonia-seawater appears to follow 2 dimensional diffusion.
3. The structural analysis based kinetic study suggests that the nickel aluminum bronze is associated with significant amount of air oxide and as the corrosion proceeds, the oxide film continues to grow. The oxide film traps the iron aluminuide/kappa (II) phase and the kappa particles tend to leave the matrix surface intact. This explains the high rate of removal of iron and aluminum in the NAB sample during corrosion.
4. The application of external stress accelerates the corrosion. However, the mechanism of corrosion remains the same (i.e. the diffusion controlled process).

REFERENCES

1. Rao, A. Srinivasa, *Mechanism on the Corrosion Product Growth on Nickel Aluminum Bronze/Ammonia or Seawater Interface: Modeling Based on Chemical Reaction Kinetics,* NSWCCD-61-TR-2006/7, Apr 2006, West Bethesda, MD.

2. Wong, C and K. L. Vasanth, "Initiation of Stress Corrosion Cracking Initiation in Nickel Aluminum Bronze", ONR FY 2004 End of Year Report.

3. Maitra, S., A. J. Pal, N. Bandhopadhaya, S. Das and J. Pal, "Use of Genetic Algorithm to Determine the Kinetic Model of Solid State Reactions", *J. Amer. Cerm. Soc*., 90[5],1611(2007).

4. Maitra, S., N. Bandhopadhaya, S. Das, A. J. Pal, and J. Pramanik.,"Non-Isothermal Decomposition Kinetics of Alakali Earth Metal Carbonates," J. Amer. Ceram. Soc., 90[4], 1299 (2007).

5. Brown, M.E., D. Dolimore and A. K. Galwey, "Reactions in the Solid Stae", pp. 340, in *Comprehensive Kinetics*, *vol. 22*, Edited by C. H. Bradford and C. F. H. Tipper, Elsiver, Amsterdam, 1980.

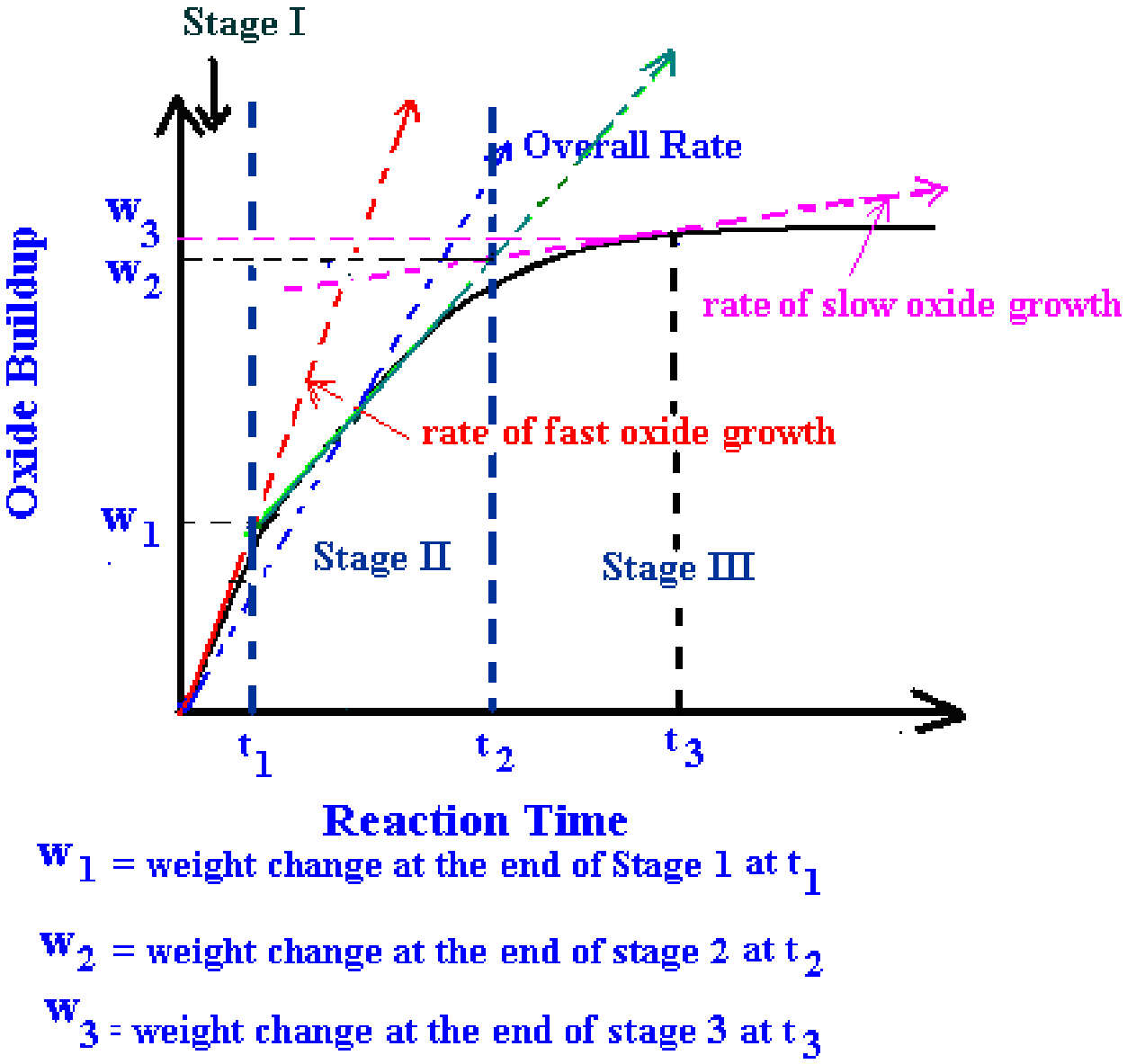

Figure 1. Schematic representation of the electrochemical reaction versus reaction time plots

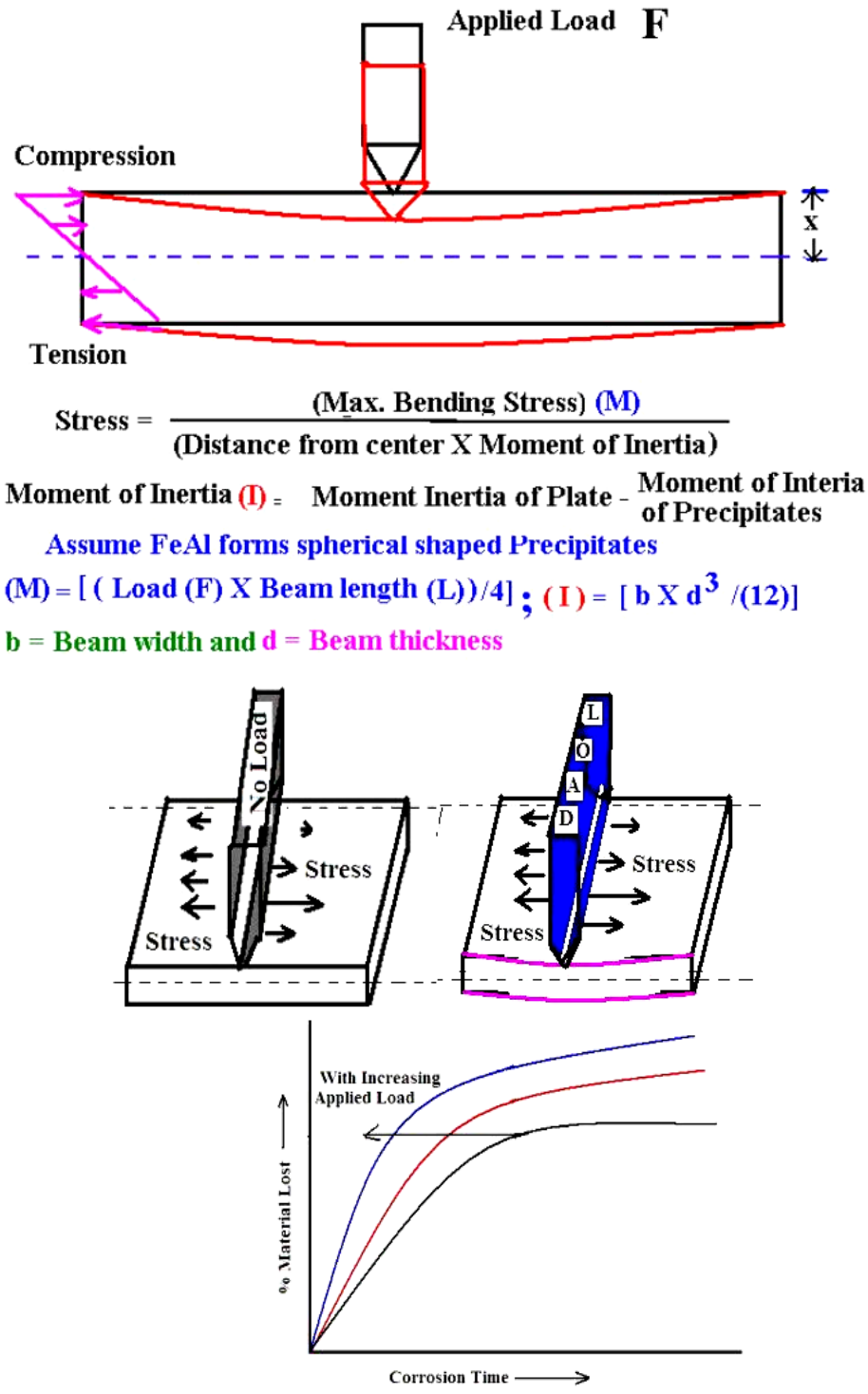

Figure 2. Schematic diagram of the stress distribution due to three point bend test and the expected material loss versus corrosion time and applied load

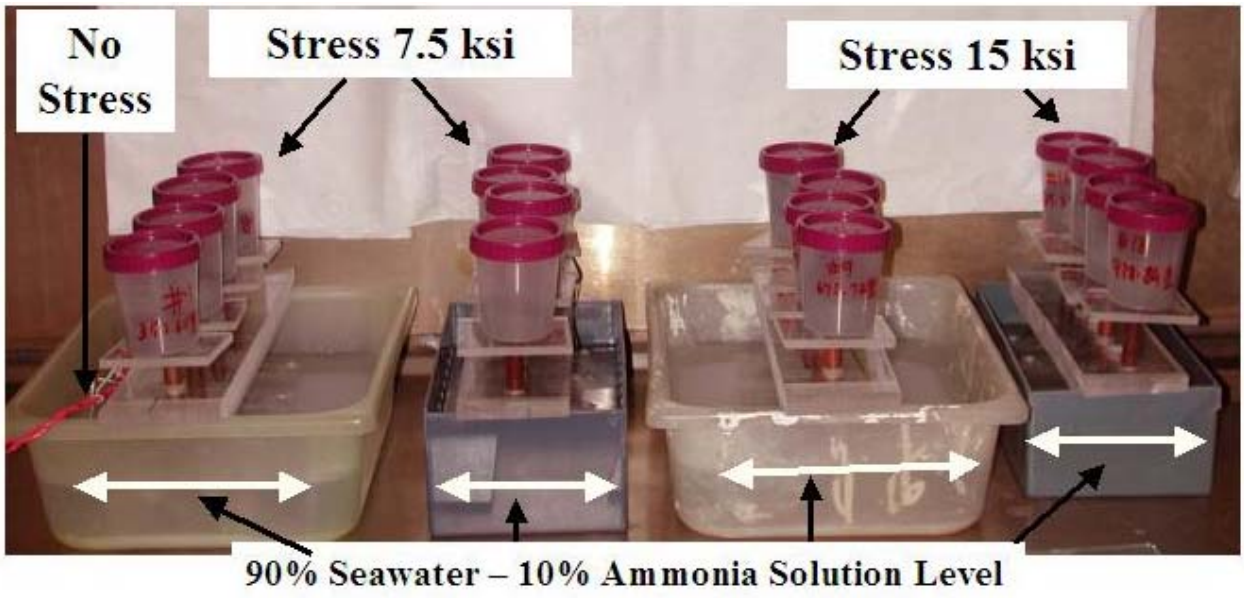

Figure 3. Typical sample and the stress corrosion testing arrangement

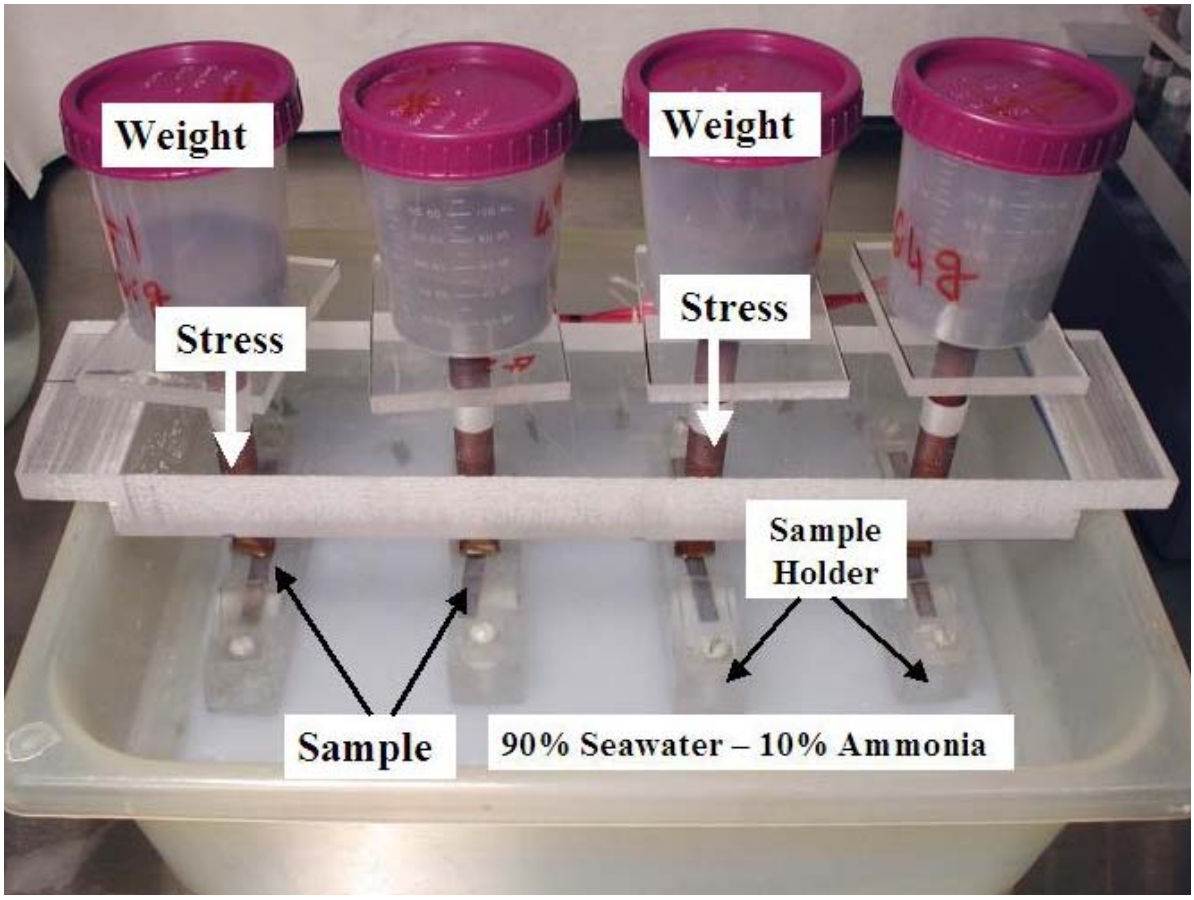

Figure 4. Typical sample and the stress corrosion testing arrangement

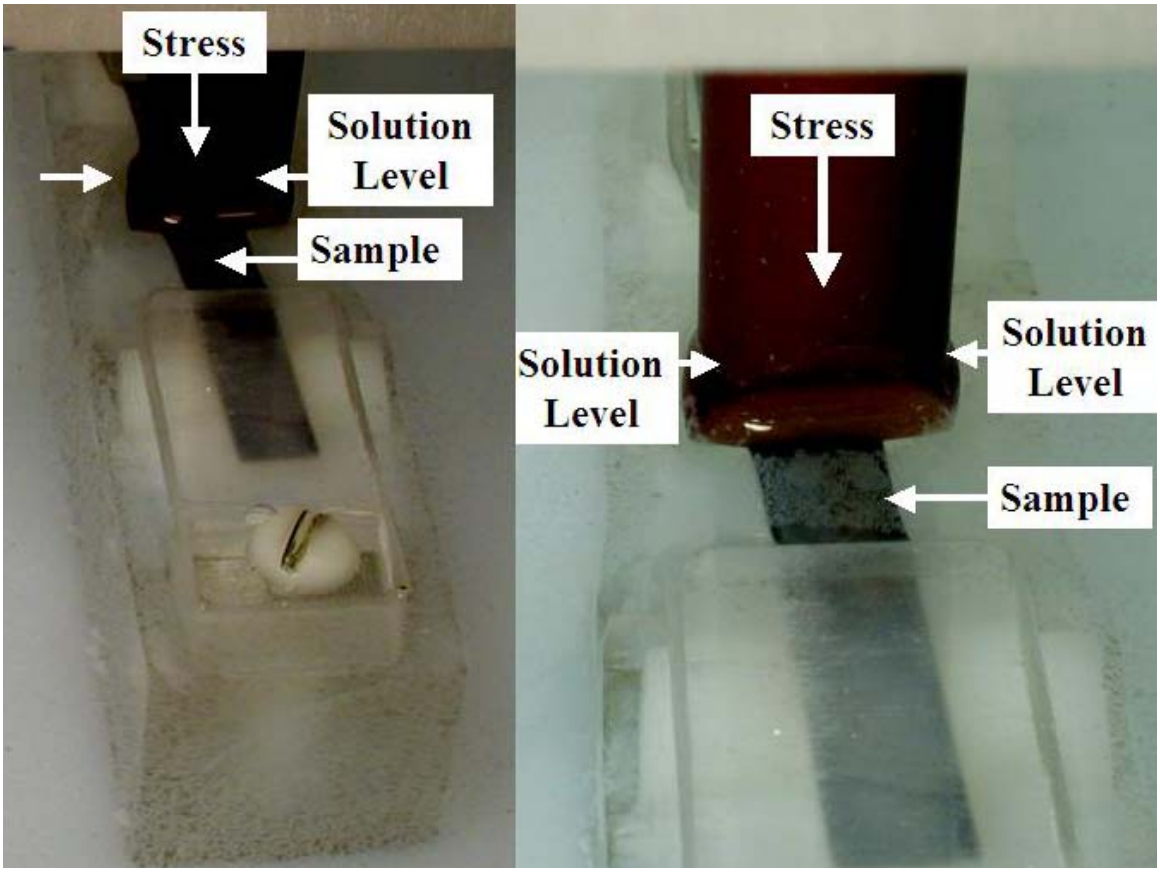

Figure 5. Typical sample and the stress corrosion testing arrangement

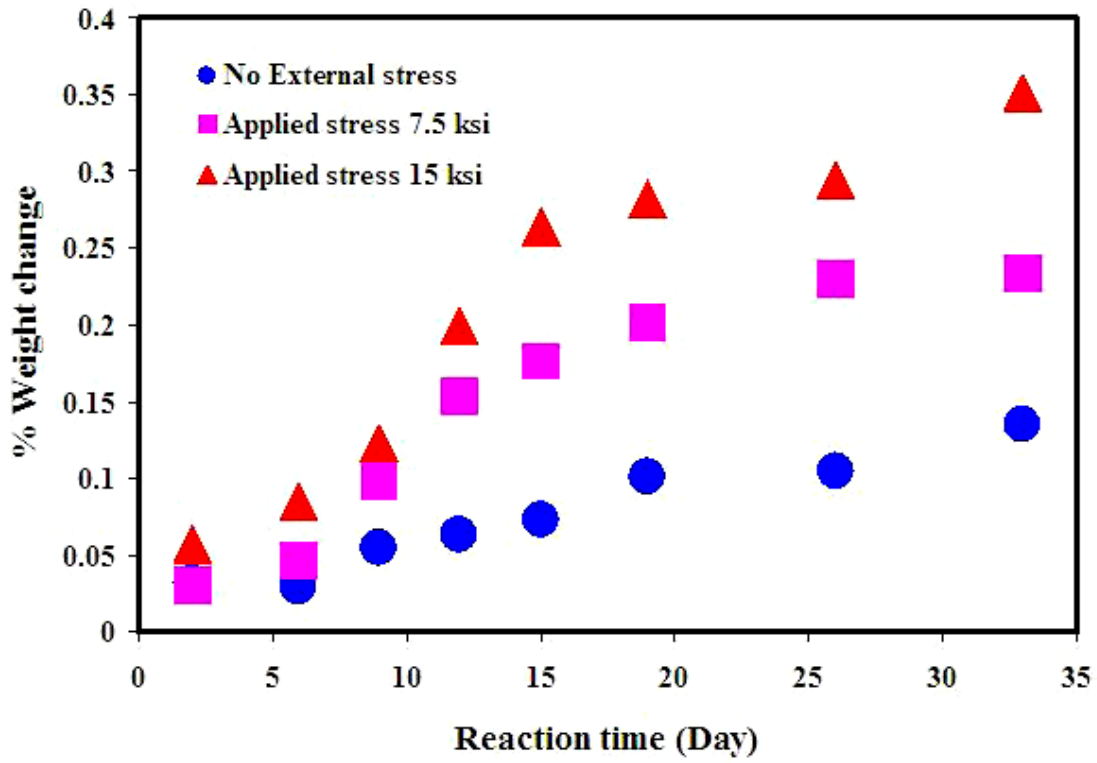

Figure 6. Comparative plot of the normalized (%) weight change versus reaction time for nickel aluminum bronze samples treated with 10% ammonia –90% seawater

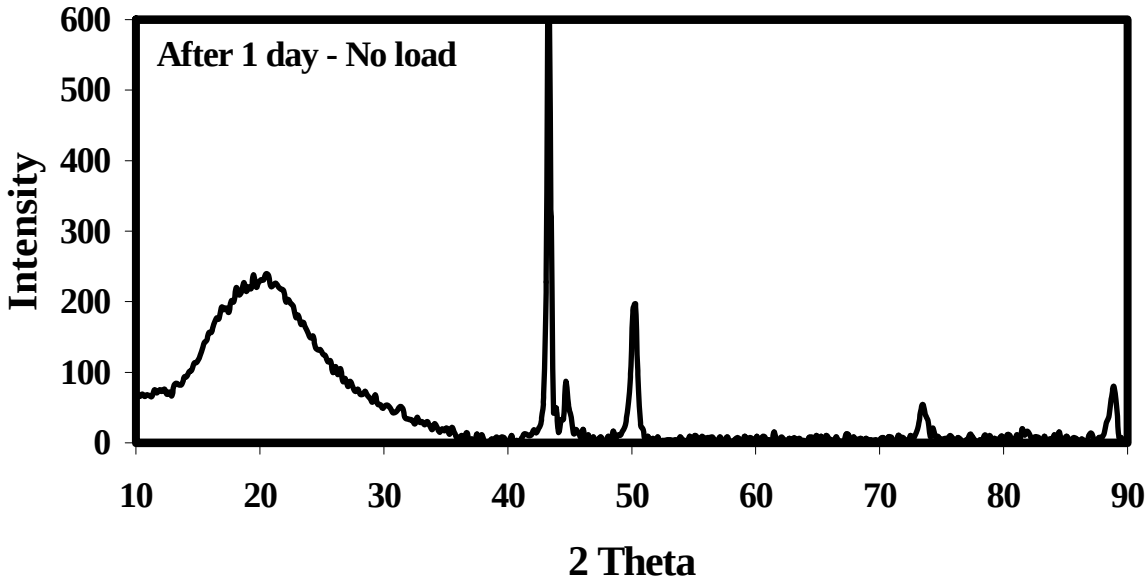

Figure 7. x ray diffraction pattern obtained from nickel aluminum bronze sample that was reacted with 10% NH_4OH-90% seawater for 1 day. NO applied external stress

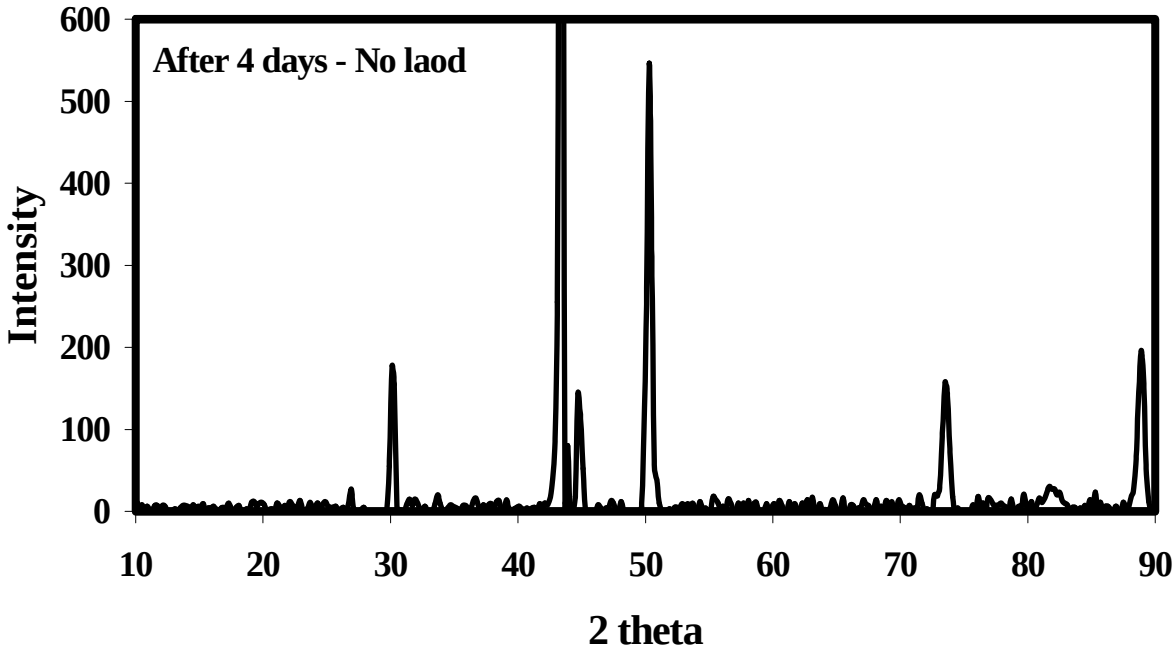

Figure 8. x ray diffraction pattern obtained from nickel aluminum bronze sample that was reacted with 10% NH_4OH-90% seawater for 4 days. NO applied external stress

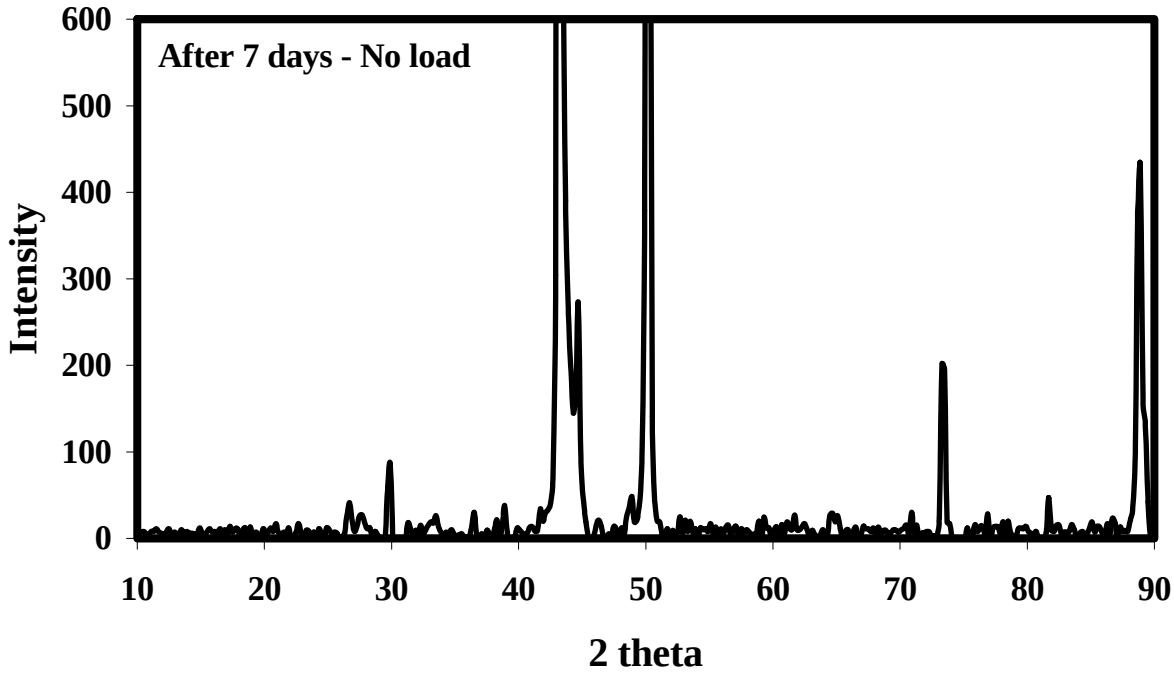

Figure 9. x ray diffraction pattern obtained from nickel aluminum bronze sample that was reacted with 10% NH_4OH-90% seawater for 7 days. NO applied external stress

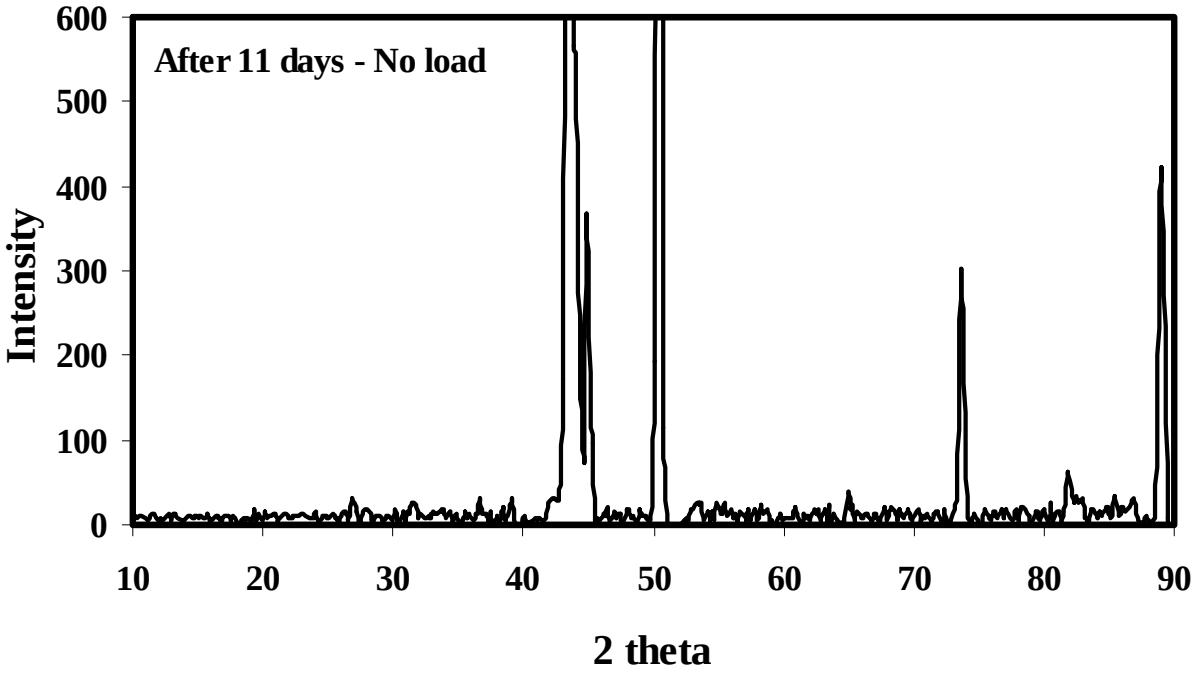

Figure 10. x ray diffraction pattern obtained from nickel aluminum bronze sample that was reacted with 10% NH_4OH-90% seawater for 11 days. NO applied external stress

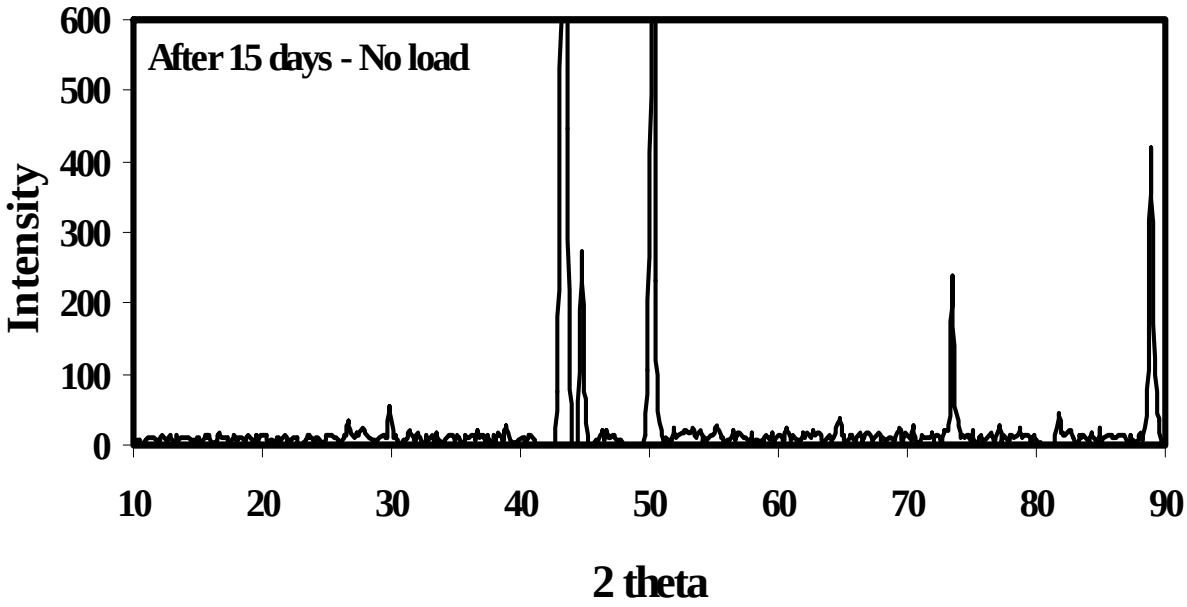

Figure 11. x ray diffraction pattern obtained from nickel aluminum bronze sample that was reacted with 10% NH_4OH-90% seawater for 15 days. NO applied external stress

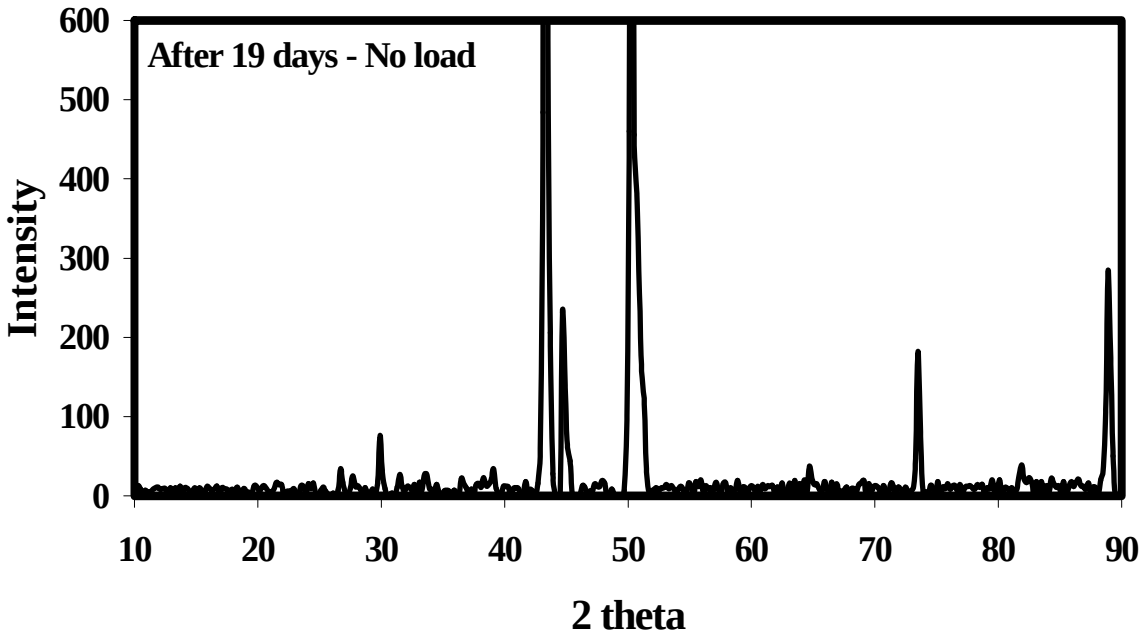

Figure 12. x ray diffraction pattern obtained from nickel aluminum bronze sample that was reacted with 10% NH_4OH-90% seawater for 19 days. NO applied external stress

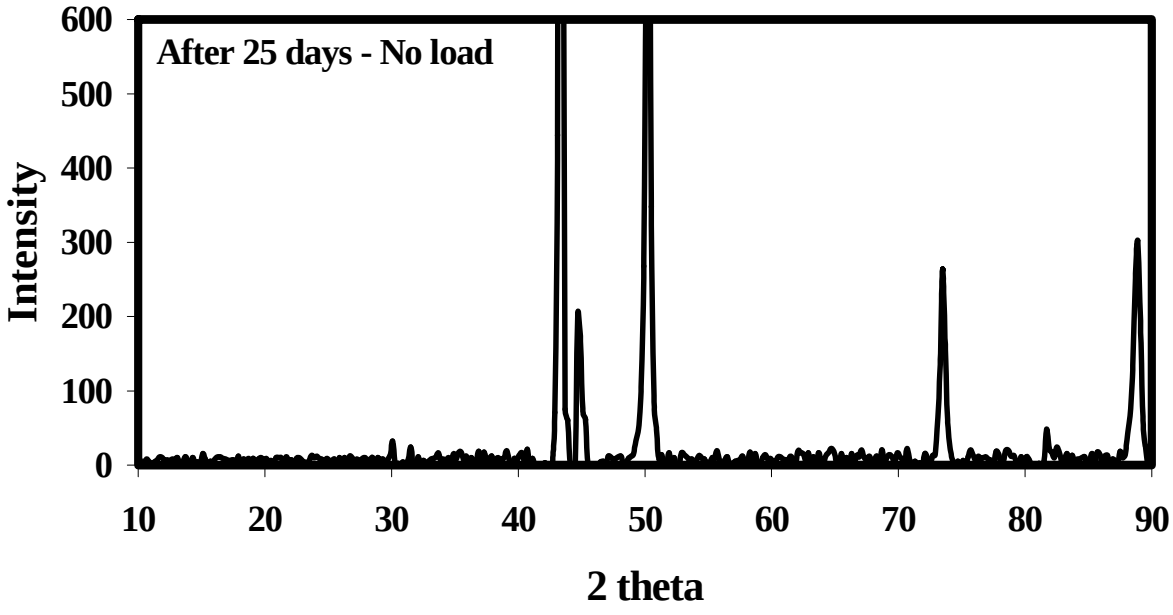

Figure 13. x ray diffraction pattern obtained from nickel aluminum bronze sample that was reacted with 10% NH_4OH-90% seawater for 25 days. NO applied external stress

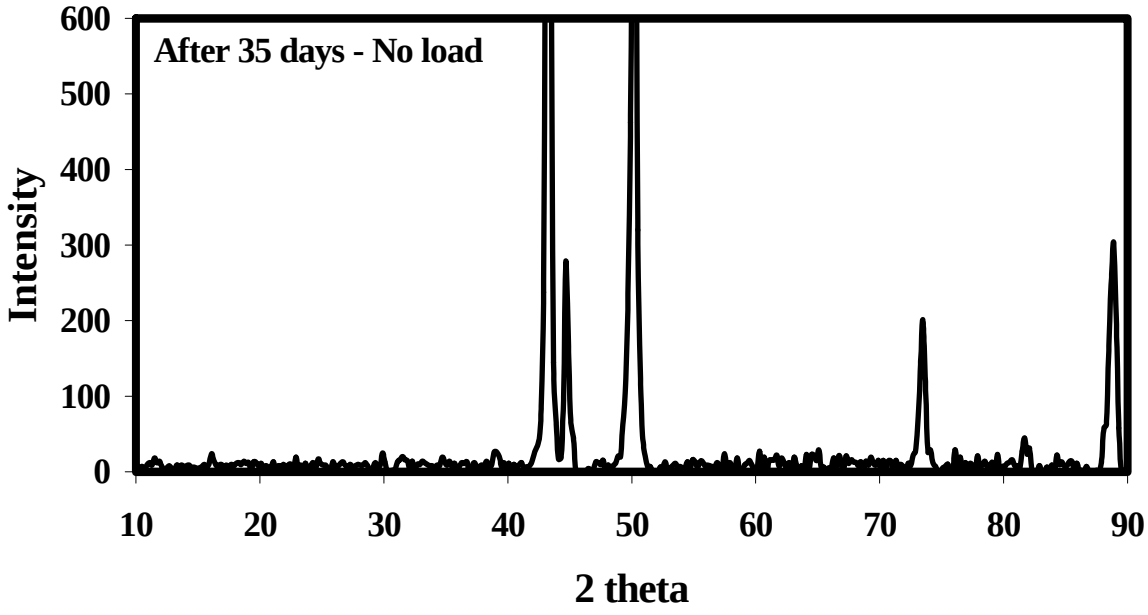

Figure 14. x ray diffraction pattern obtained from nickel aluminum bronze sample that was reacted with 10% NH_4OH-90% seawater for 35 days. NO applied external stress

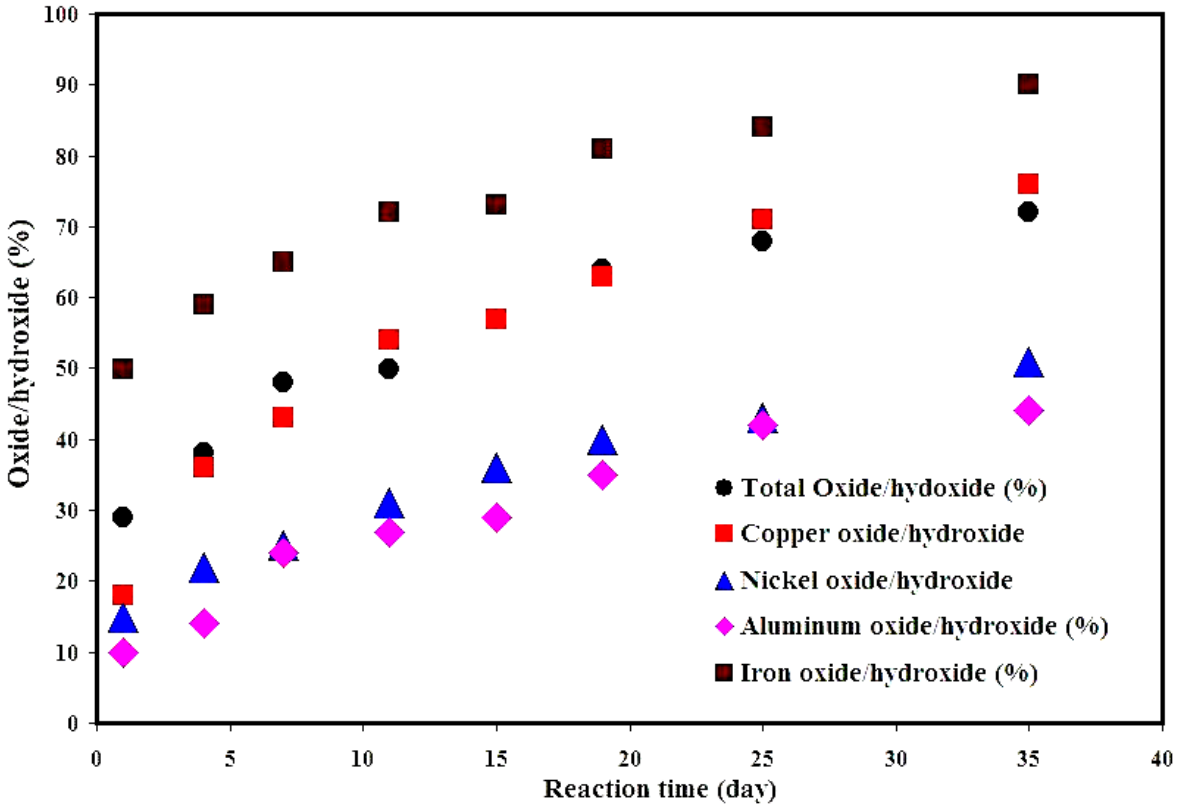

Figure 15 Comparative plot of oxides/hydroxides formed on nickel aluminum bronze surface due to corrosion in 10 ammonia-90% seawater. No external applied stress

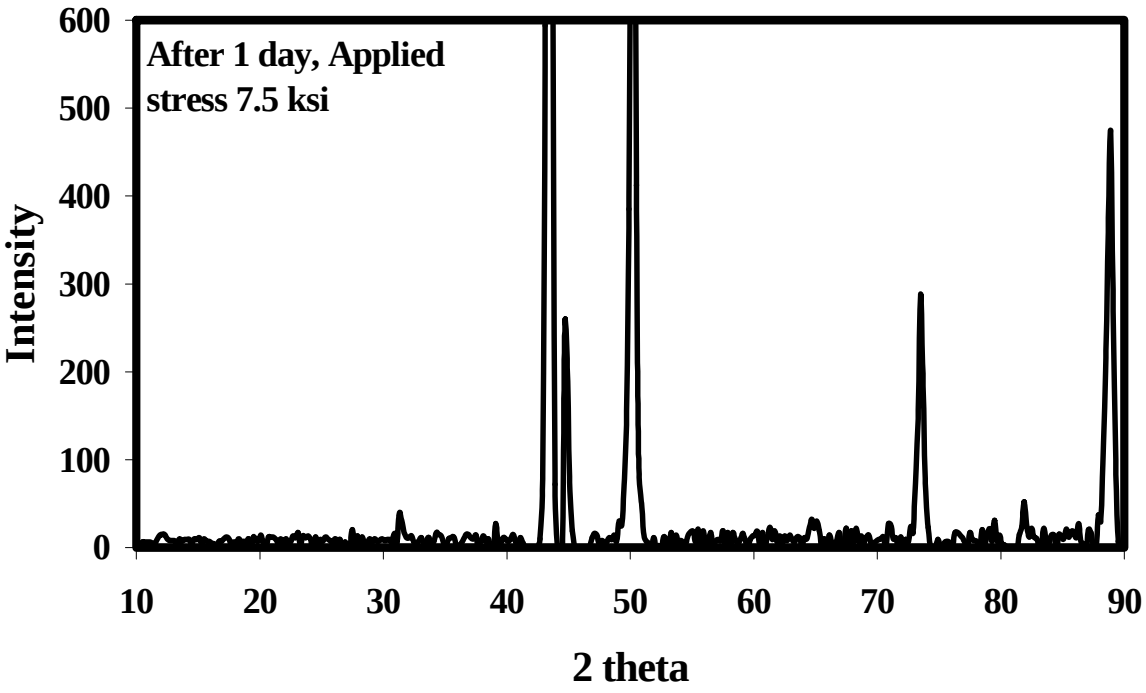

Figure 16. x ray diffraction pattern obtained from nickel aluminum bronze sample that was reacted with 10% NH_4OH-90% seawater for 1 day. Applied external stress 7.5 ksi

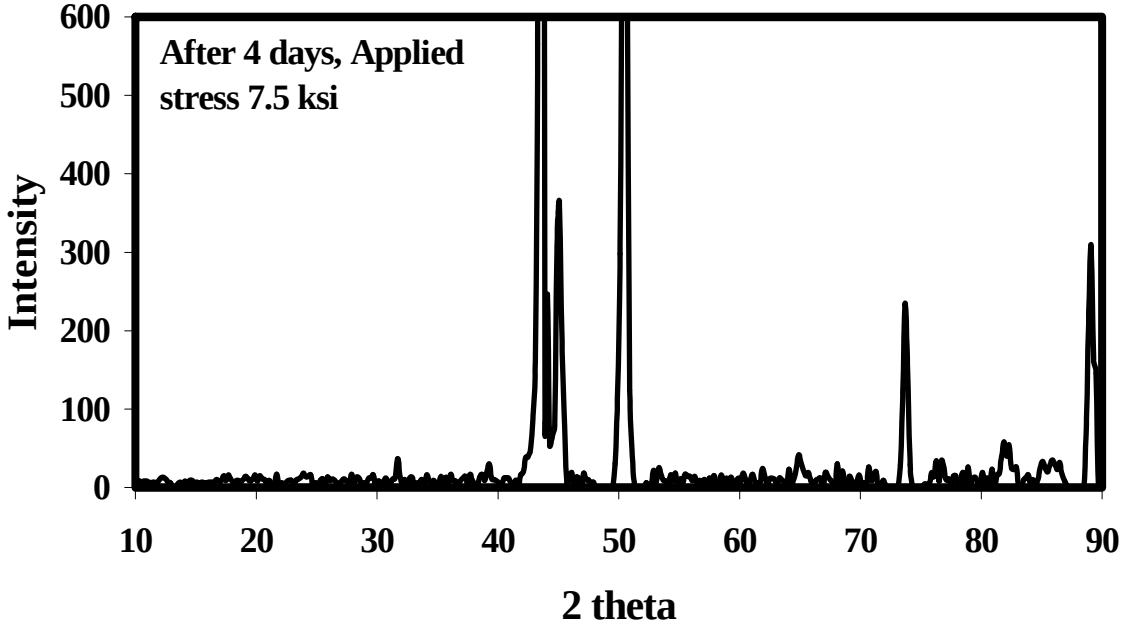

Figure 17. x ray diffraction pattern obtained from nickel aluminum bronze sample that was reacted with 10% NH_4OH-90% seawater for 4 days. Applied external stress 7.5 ksi

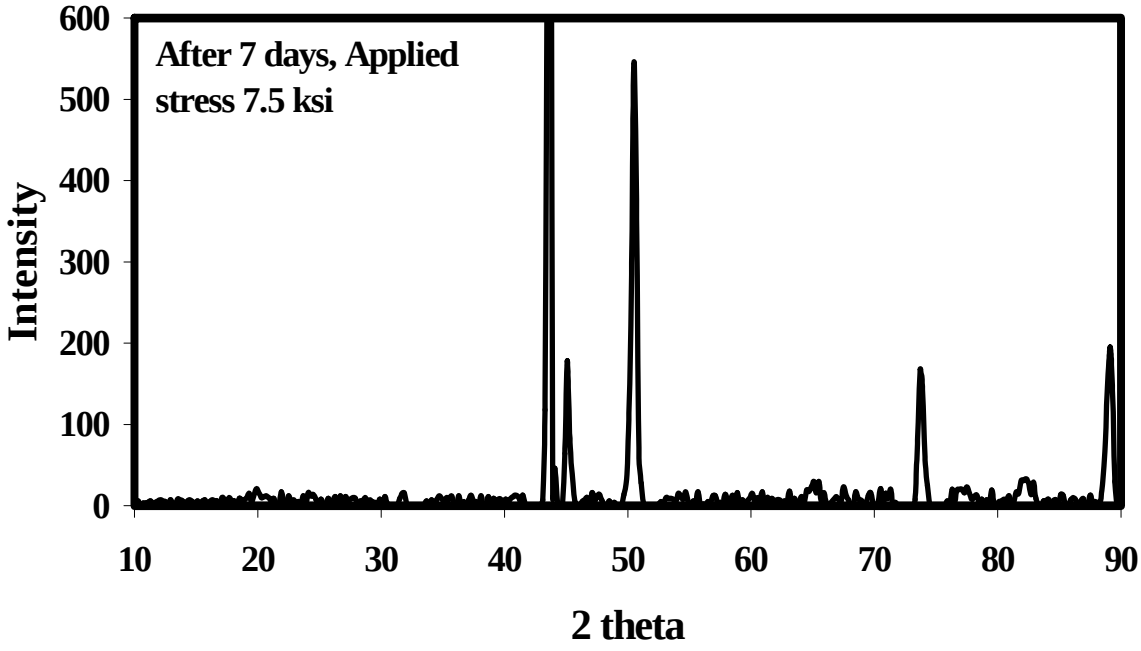

Figure 18. x ray diffraction pattern obtained from nickel aluminum bronze sample that was reacted with 10% NH_4OH-90% seawater for 7 days. Applied external stress 7.5 ksi

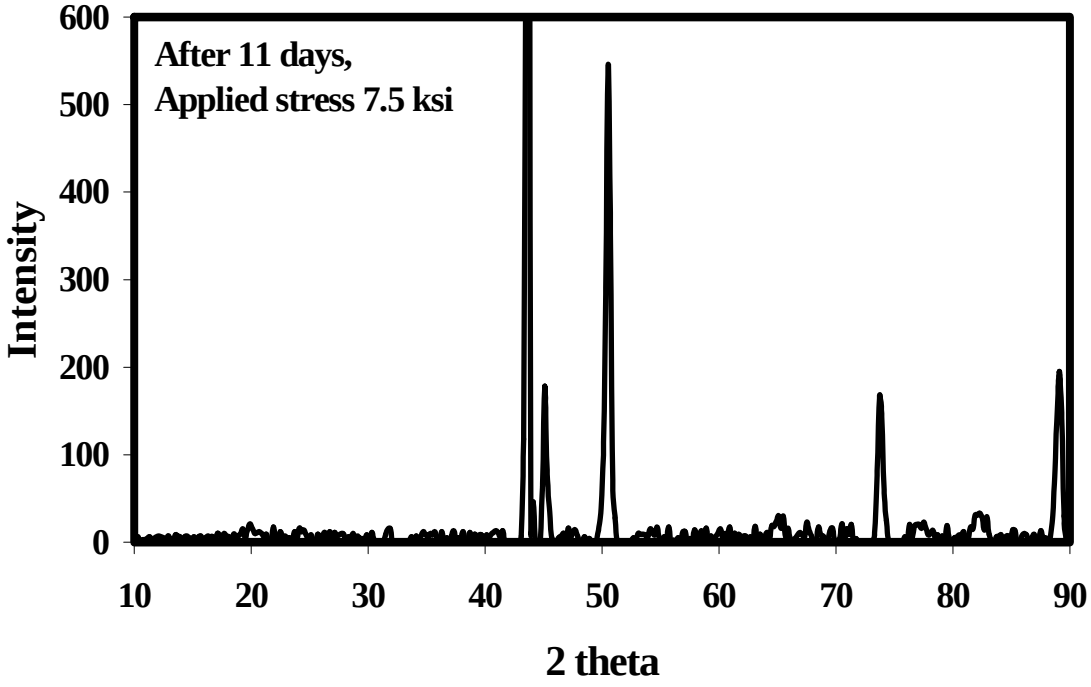

Figure 19. x ray diffraction pattern obtained from nickel aluminum bronze sample that was reacted with 10% NH_4OH-90% seawater for 11 days. Applied external stress 7.5 ksi

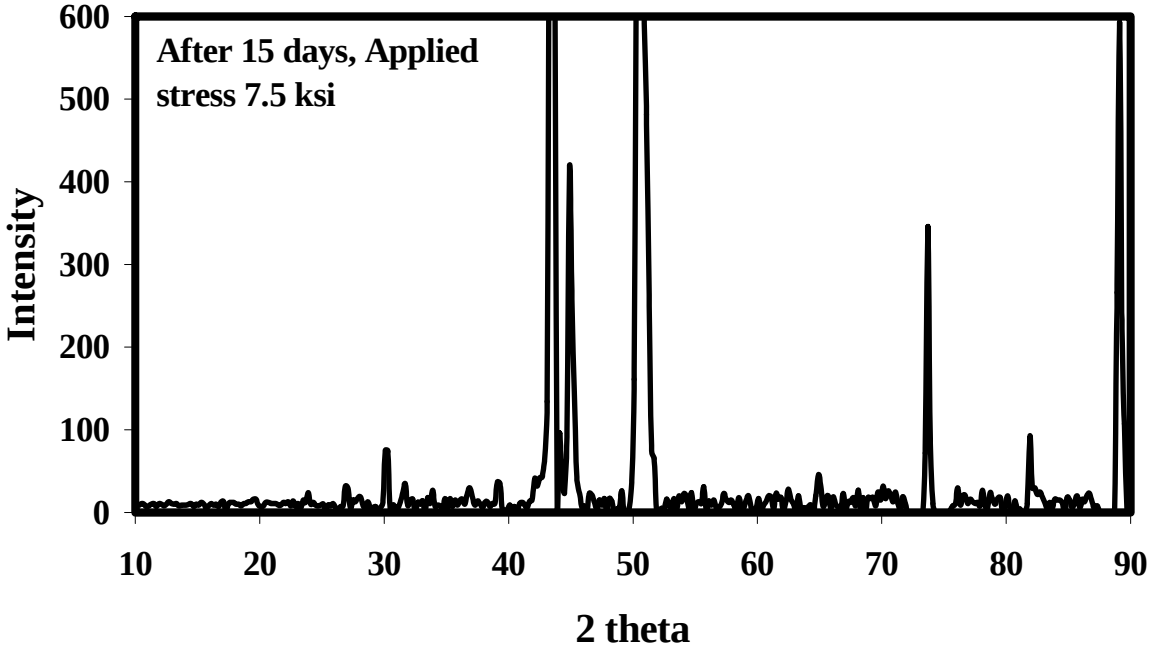

Figure 20. x ray diffraction pattern obtained from nickel aluminum bronze sample that was reacted with 10% NH_4OH-90% seawater for 15 days. Applied external stress 7.5 ksi

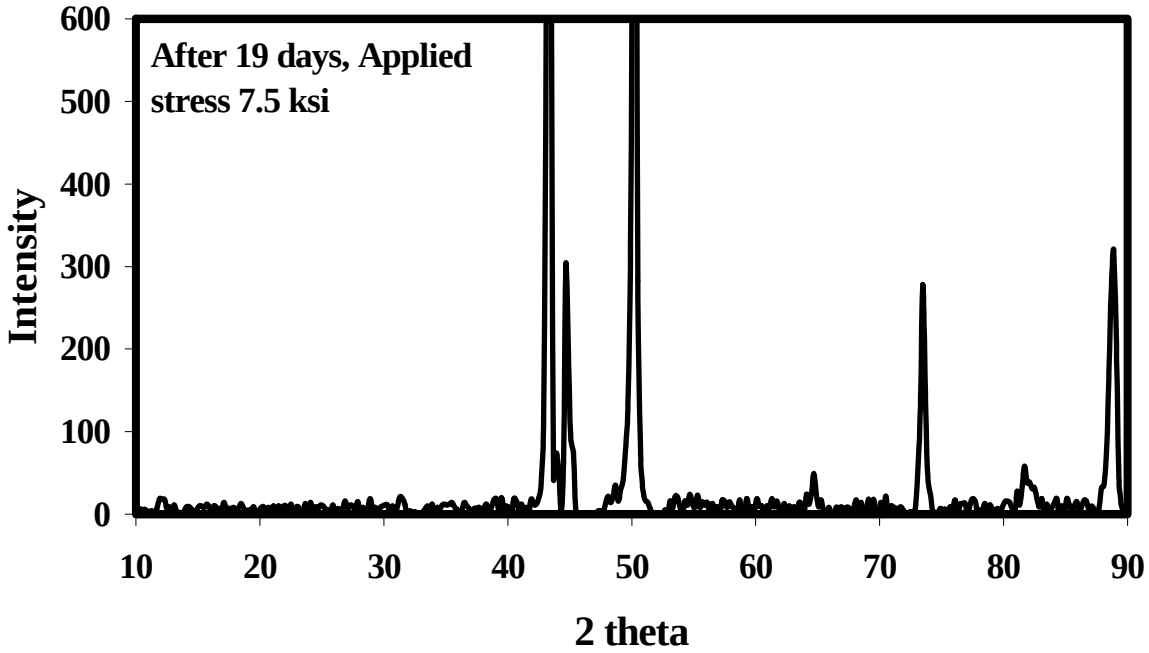

Figure 21. x ray diffraction pattern obtained from nickel aluminum bronze sample that was reacted with 10% NH_4OH-90% seawater for 19 days. Applied external stress 7.5 ksi

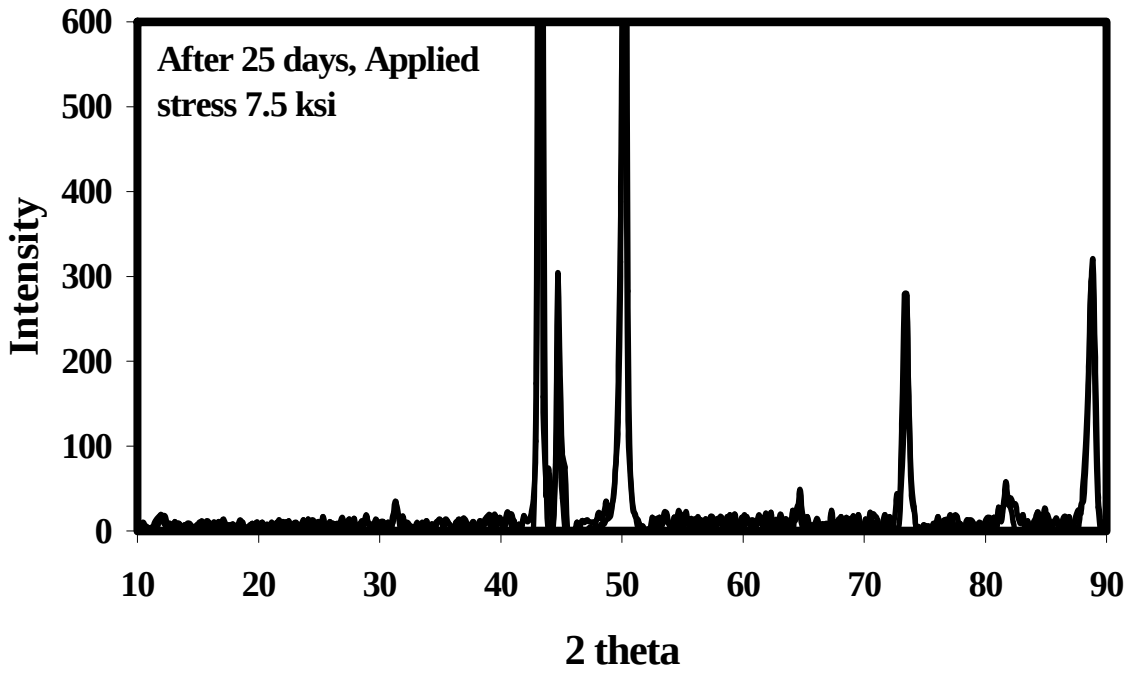

Figure 22. x ray diffraction pattern obtained from nickel aluminum bronze sample that was reacted with 10% NH_4OH-90% seawater for 25 days. Applied external stress 7.5 ksi

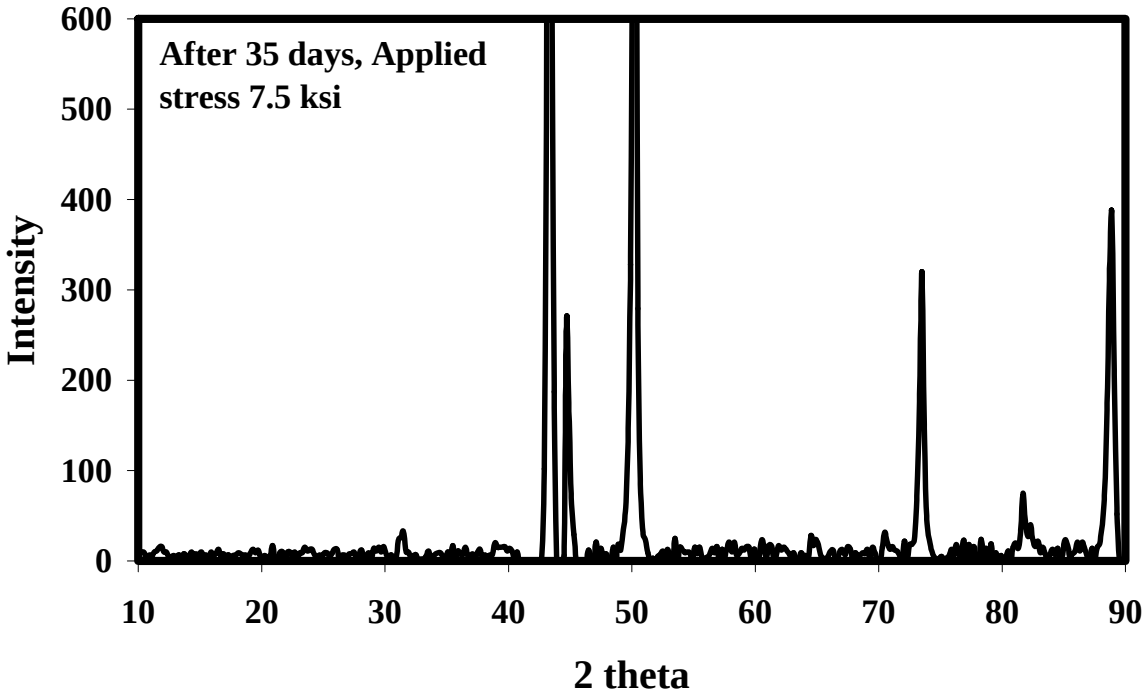

Figure 23. x ray diffraction pattern obtained from nickel aluminum bronze sample that was reacted with 10% NH_4OH-90% seawater for 35 days. Applied external stress 7.5 ksi

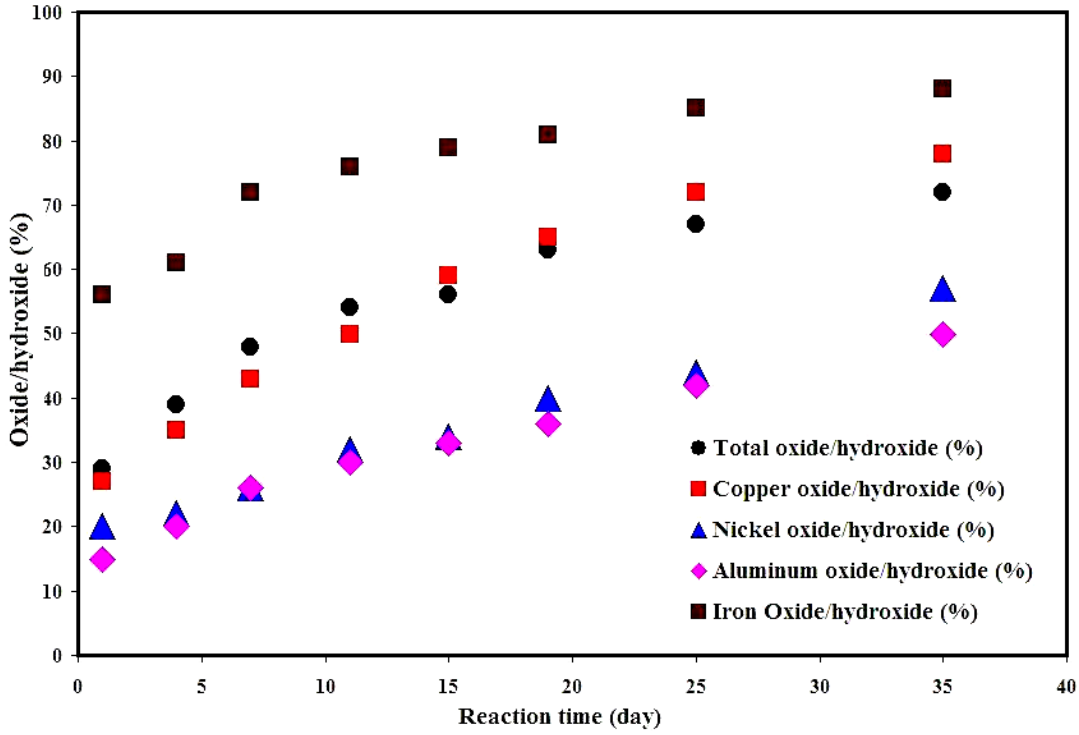

Figure 24. Comparative plot of oxides/hydroxides formed on nickel aluminum bronze surface due to corrosion in 10% ammonia-90% seawater. Applied external stress 7.5 ksi

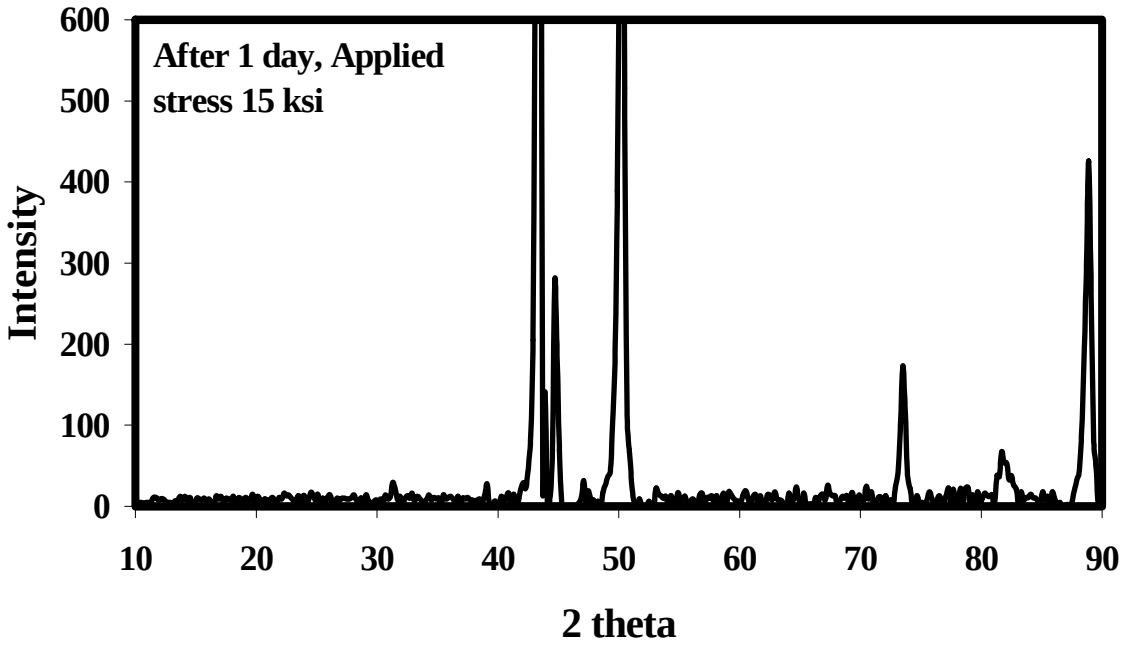

Figure 25. x ray diffraction pattern obtained from nickel aluminum bronze sample that was reacted with 10% NH_4OH-90% seawater for 1 day. Applied external stress 15 ksi

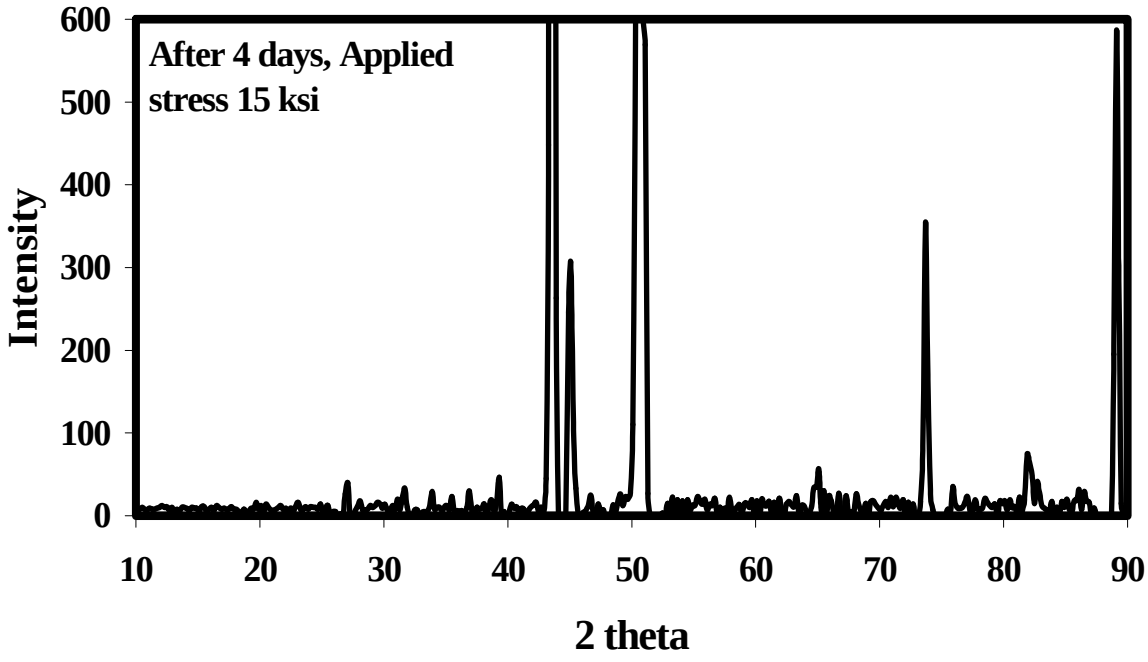

Figure 26. x ray diffraction pattern obtained from nickel aluminum bronze sample that was reacted with 10% NH_4OH-90% seawater for 4 days. Applied external stress 15 ksi

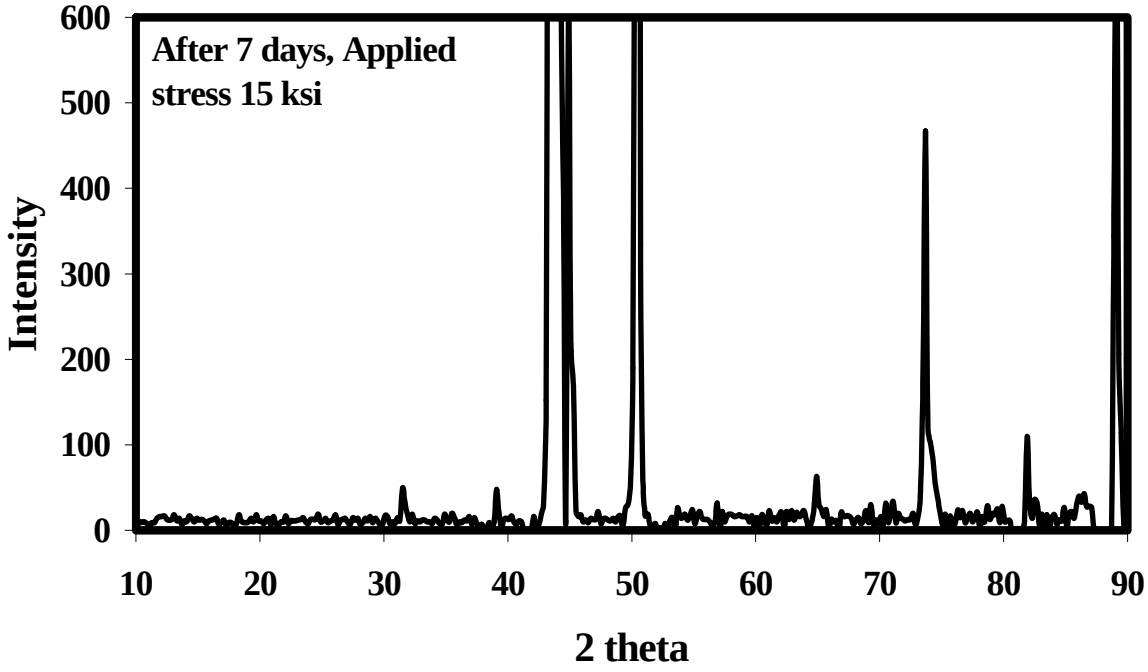

Figure 27. x ray diffraction pattern obtained from nickel aluminum bronze sample that was reacted with 10% NH_4OH-90% seawater for 7 days. Applied external stress 15 ksi

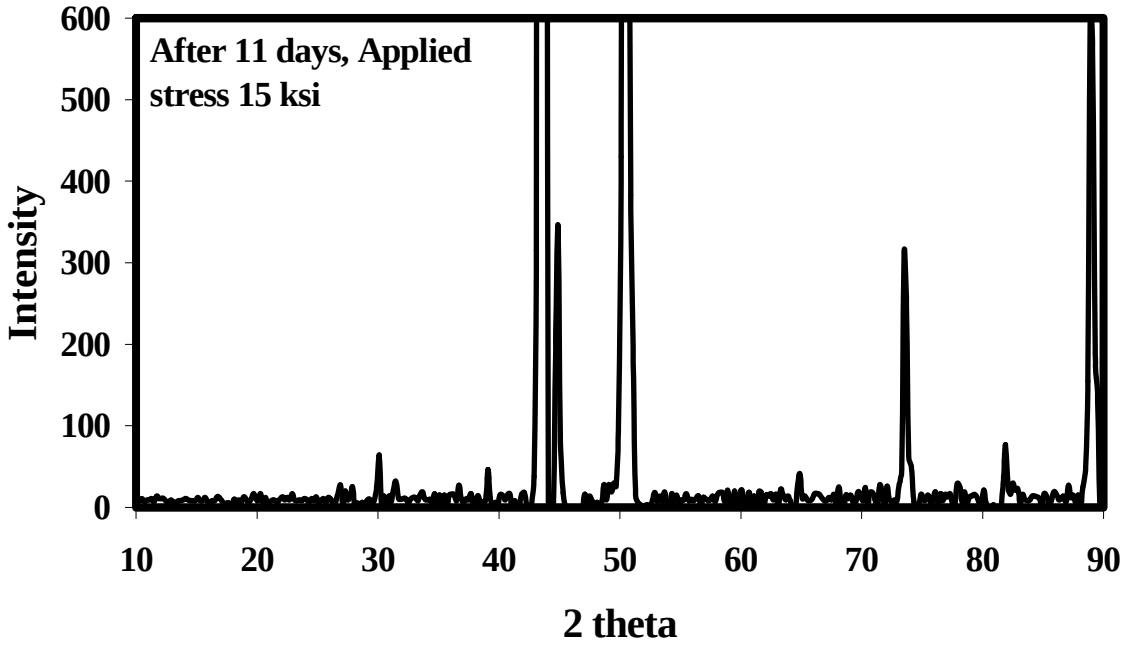

Figure 28. x ray diffraction pattern obtained from nickel aluminum bronze sample that was reacted with 10% NH_4OH-90% seawater for 11 days. Applied external stress 15 ksi

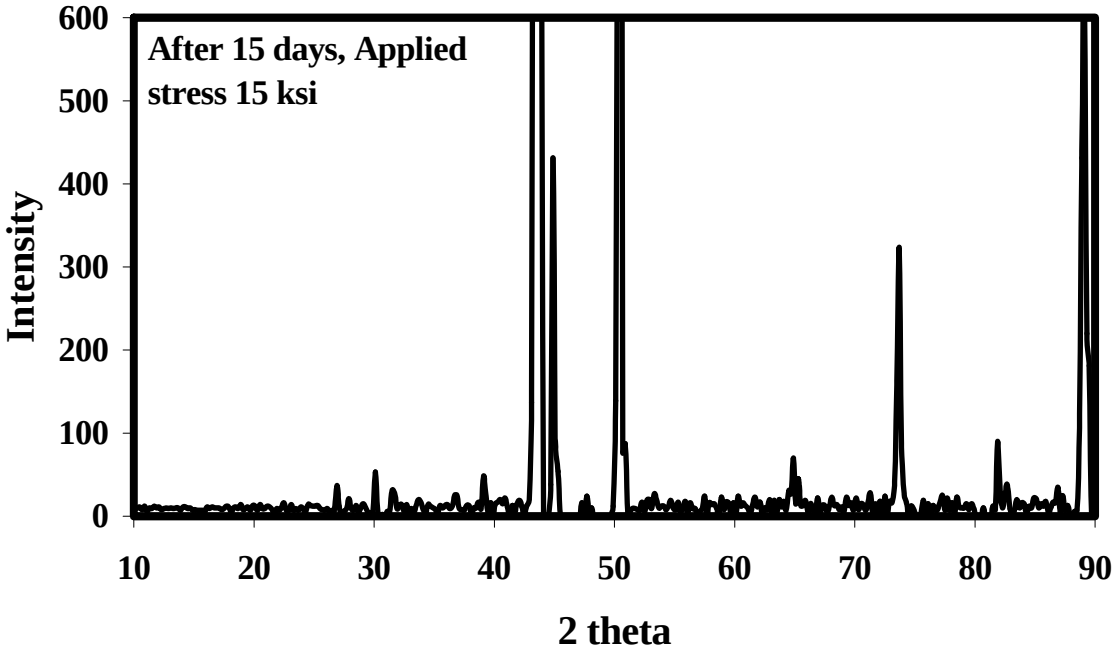

Figure 29. x ray diffraction pattern obtained from nickel aluminum bronze sample that was reacted with 10% NH_4OH-90% seawater for 15 days. Applied external stress 15 ksi

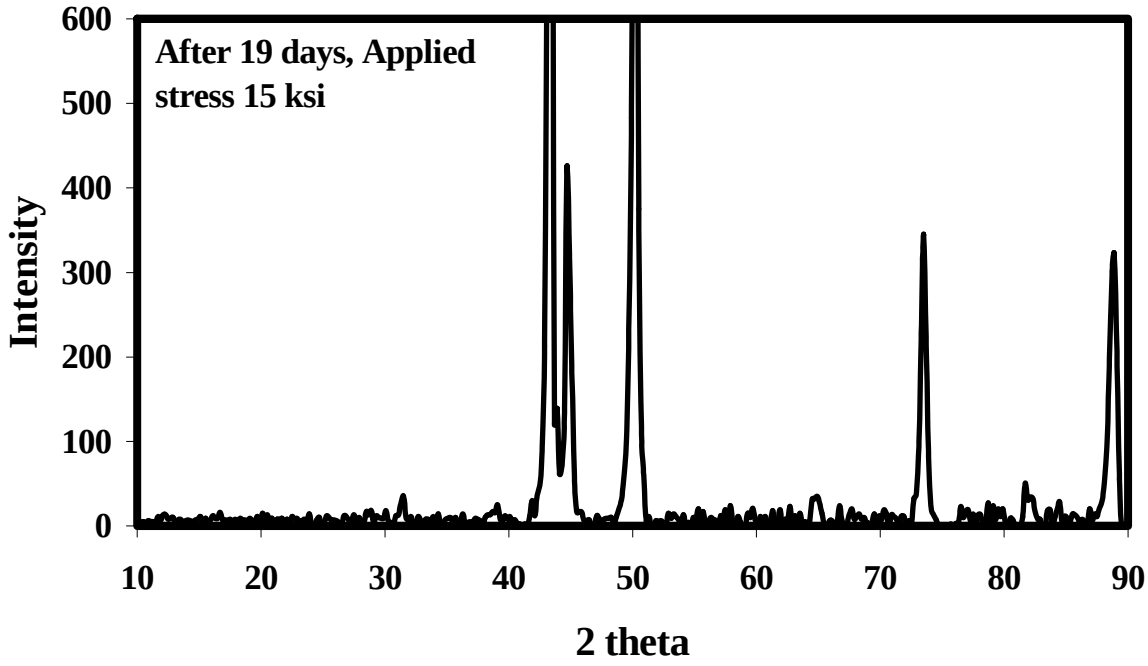

Figure 30. x ray diffraction pattern obtained from nickel aluminum bronze sample that was reacted with 10% NH_4OH-90% seawater for 19 days. Applied external stress 15 ksi

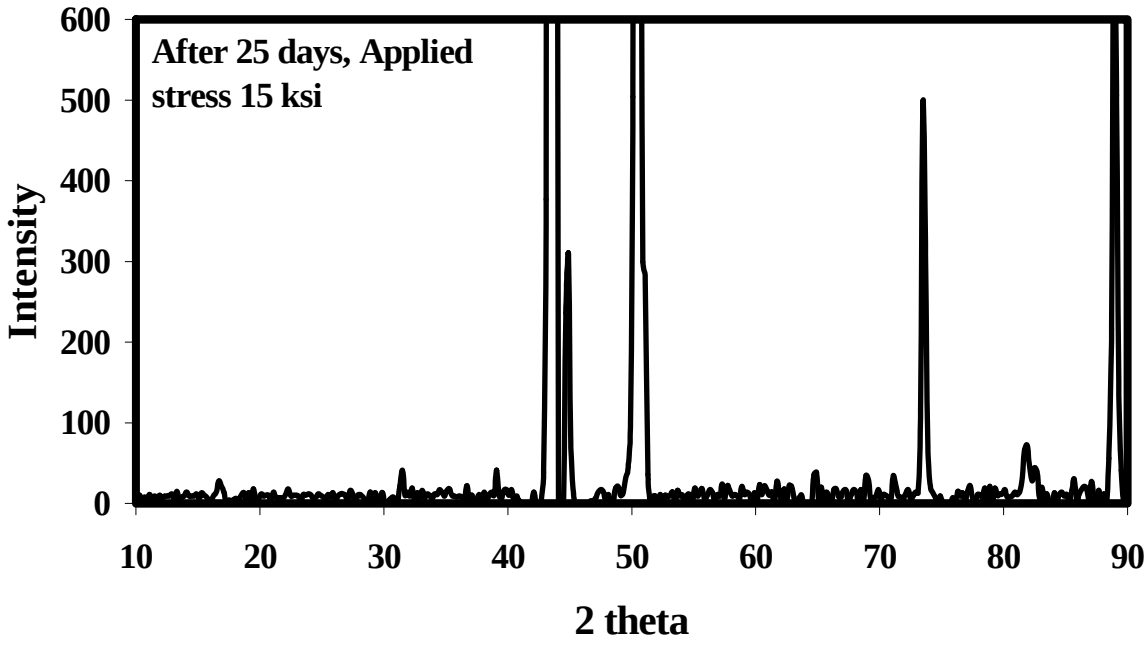

Figure 31. x ray diffraction pattern obtained from nickel aluminum bronze sample that was reacted with 10% NH_4OH-90% seawater for 25 days. Applied external stress 15 ksi

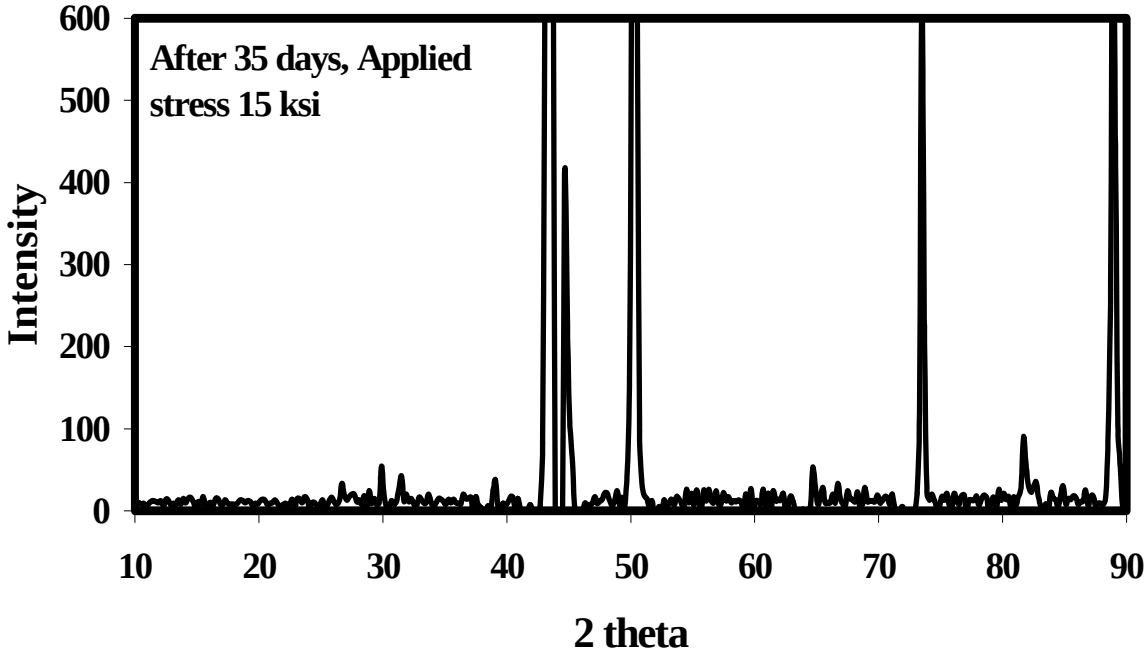

Figure 32. x ray diffraction pattern obtained from nickel aluminum bronze sample that was reacted with 10% NH_4OH-90% seawater for 35 days. Applied external stress 15 ksi

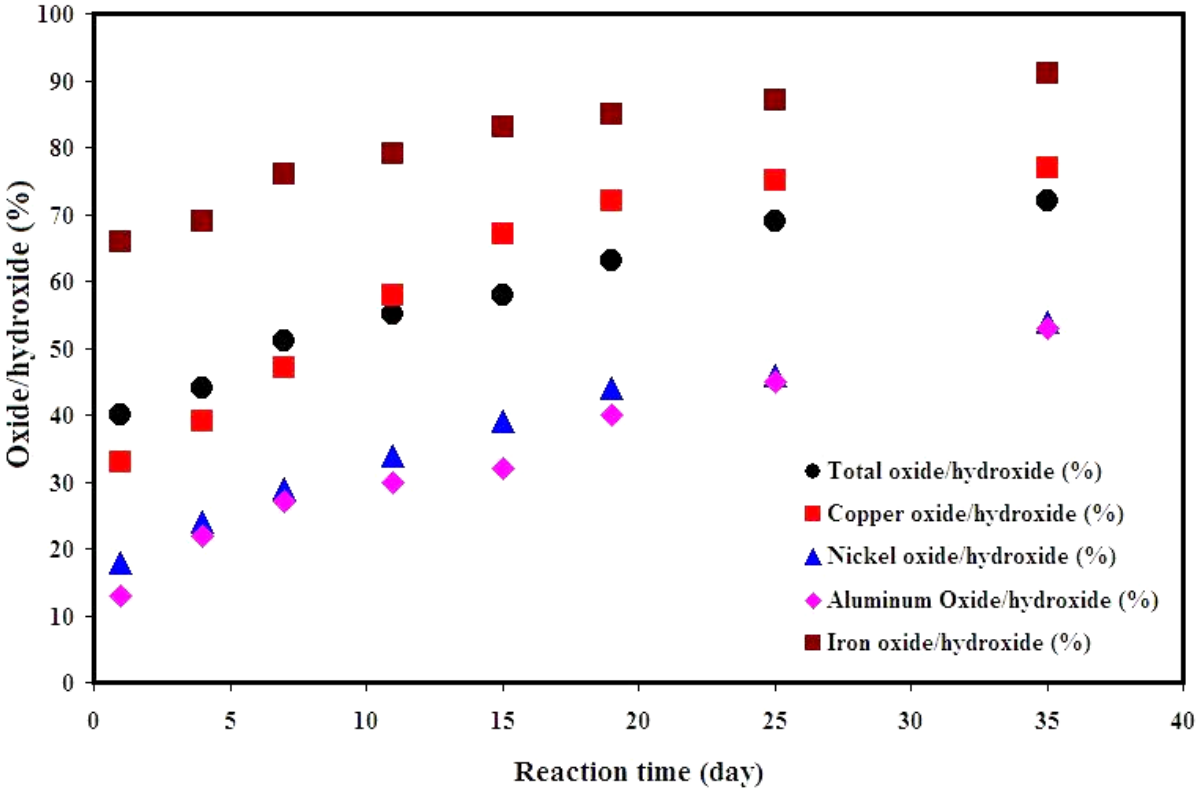

Figure 33. Comparative plot of oxides/hydroxides formed on nickel aluminum bronze surface due to corrosion in 10% ammonia-90% seawater. Applied external stress 15 ksi

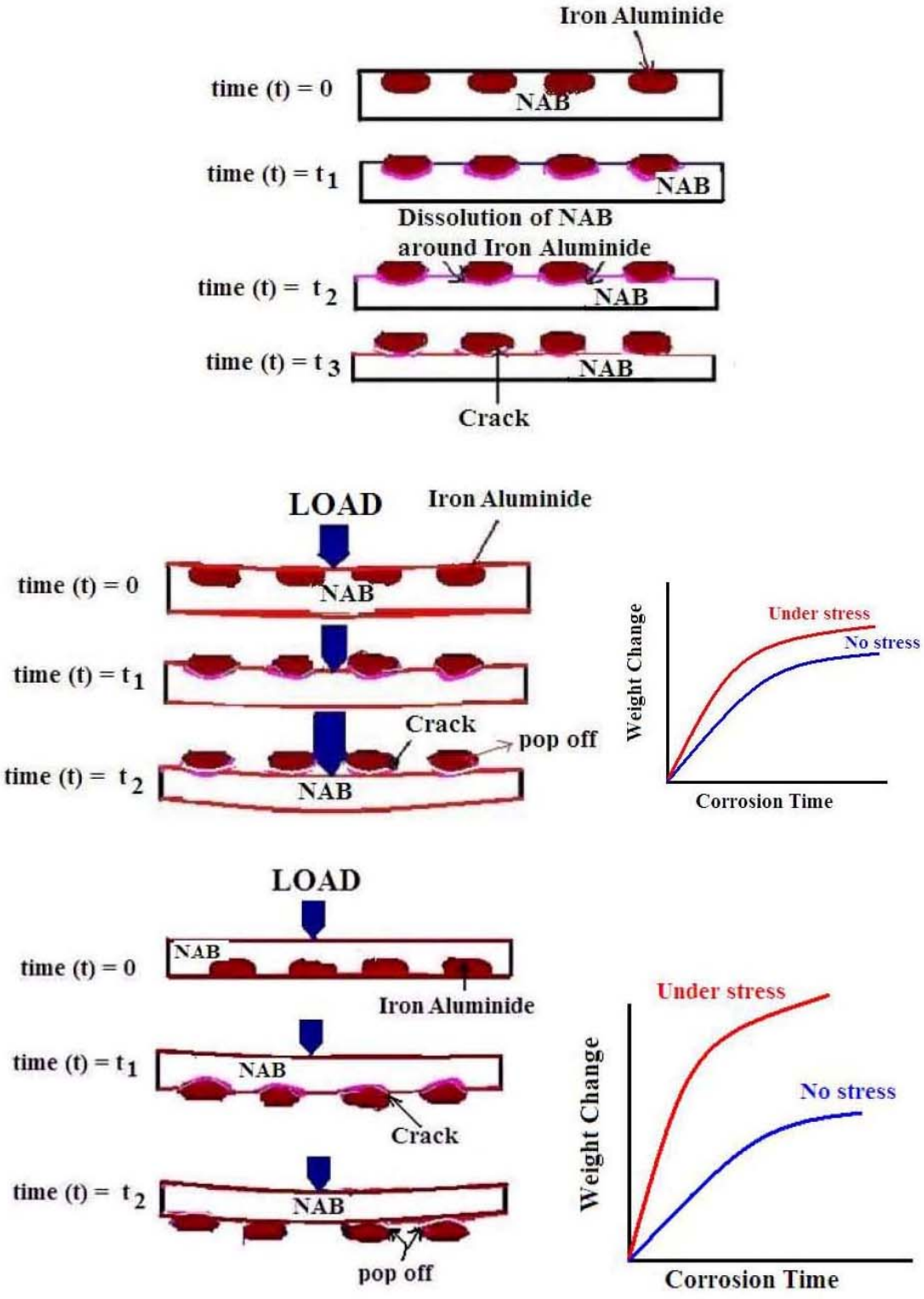

Figure 34. Schematic representation of iron aluminide embedded in NAB matrix

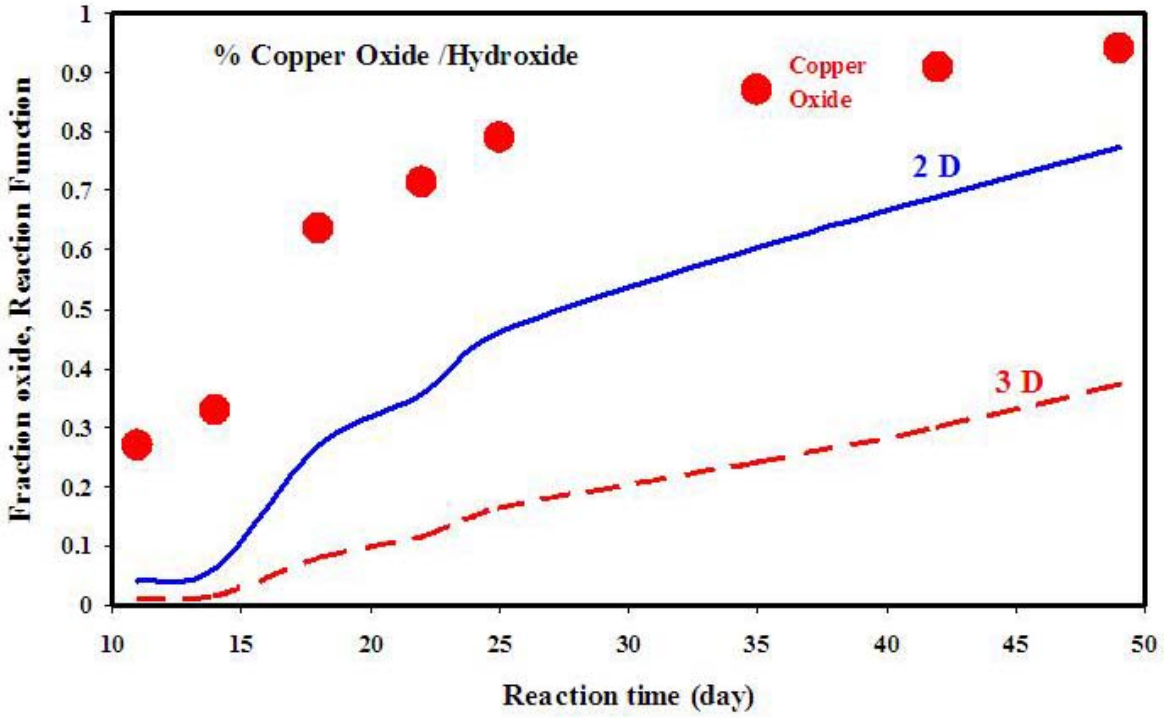

Figure 35. % Copper oxide/hydroxides on the surface of nickel aluminum bronze (NAB) in 10% ammonia and 90% seawater. Symbol represents estimation based on experimental values, 2D and 3D represents the predictions based on 2-dimensional and 3-dimensional diffusion models

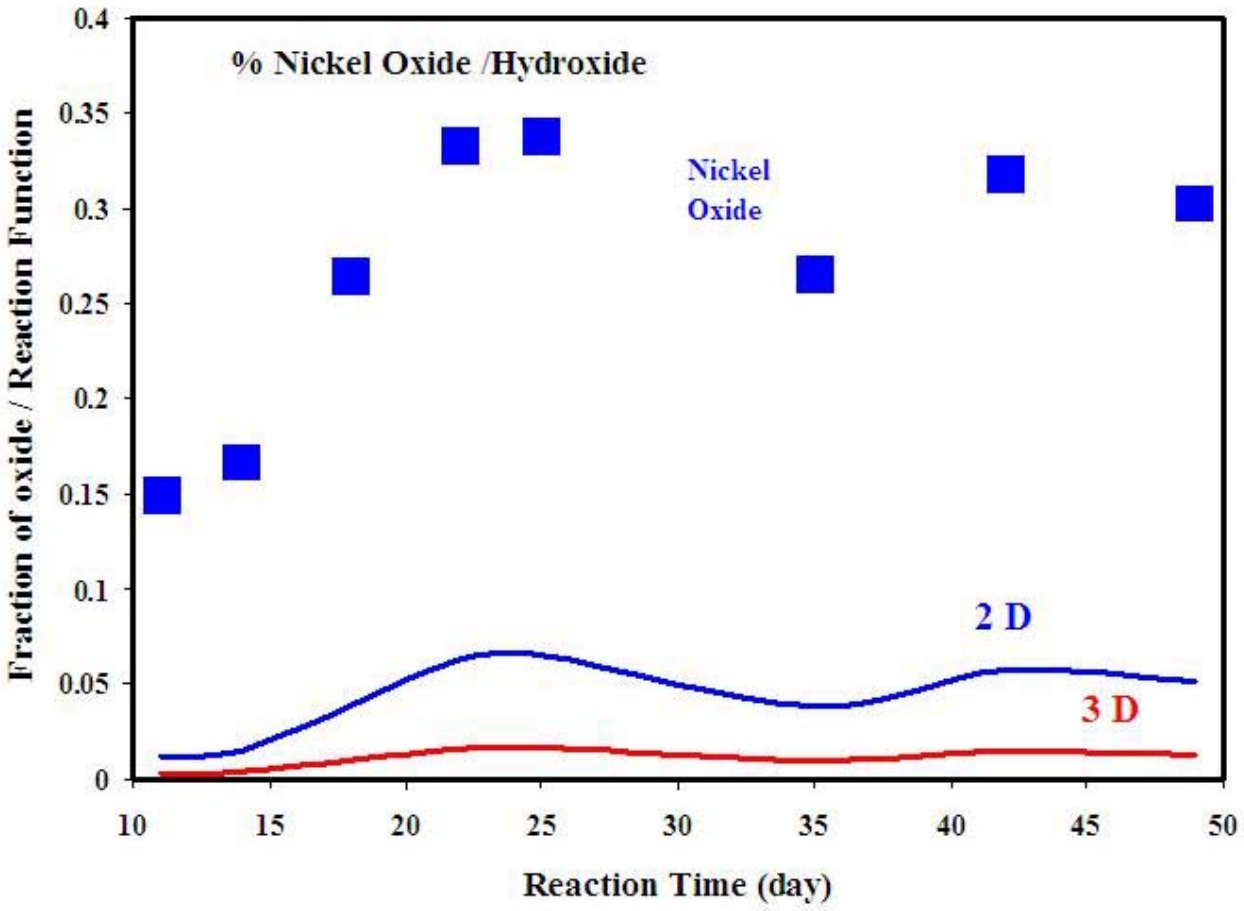

Figure 36. % Nickel oxide/hydroxides on the surface of nickel aluminum bronze (NAB) in 10% ammonia and 90% seawater. Symbol represents estimation based on experimental values, 2D and 3D represents the predictions based on 2-dimensional and 3-dimensional diffusion models

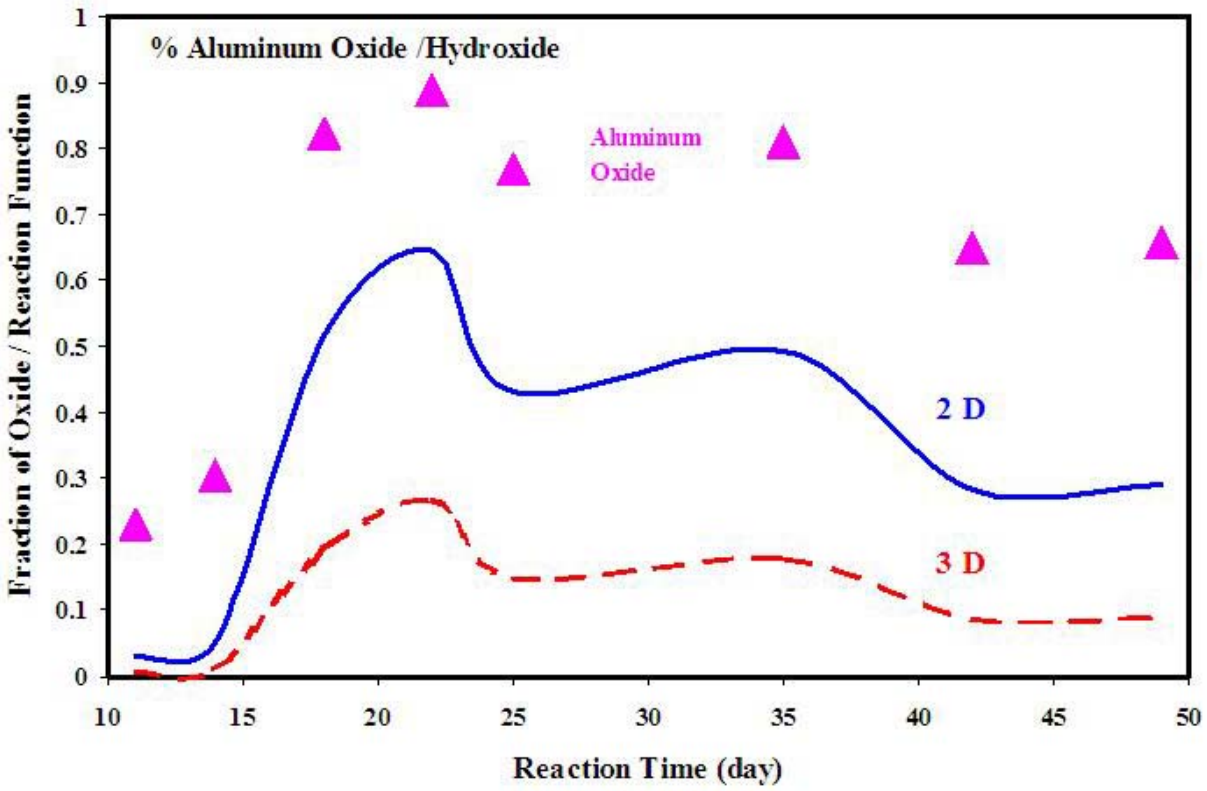

Figure 37. % Aluminum oxide/hydroxides on the surface of nickel aluminum bronze (NAB) in 10% ammonia and 90% seawater. Symbol represents estimation based on experimental values, 2D and 3D represents the predictions based on 2-dimensional and 3-dimensional diffusion models

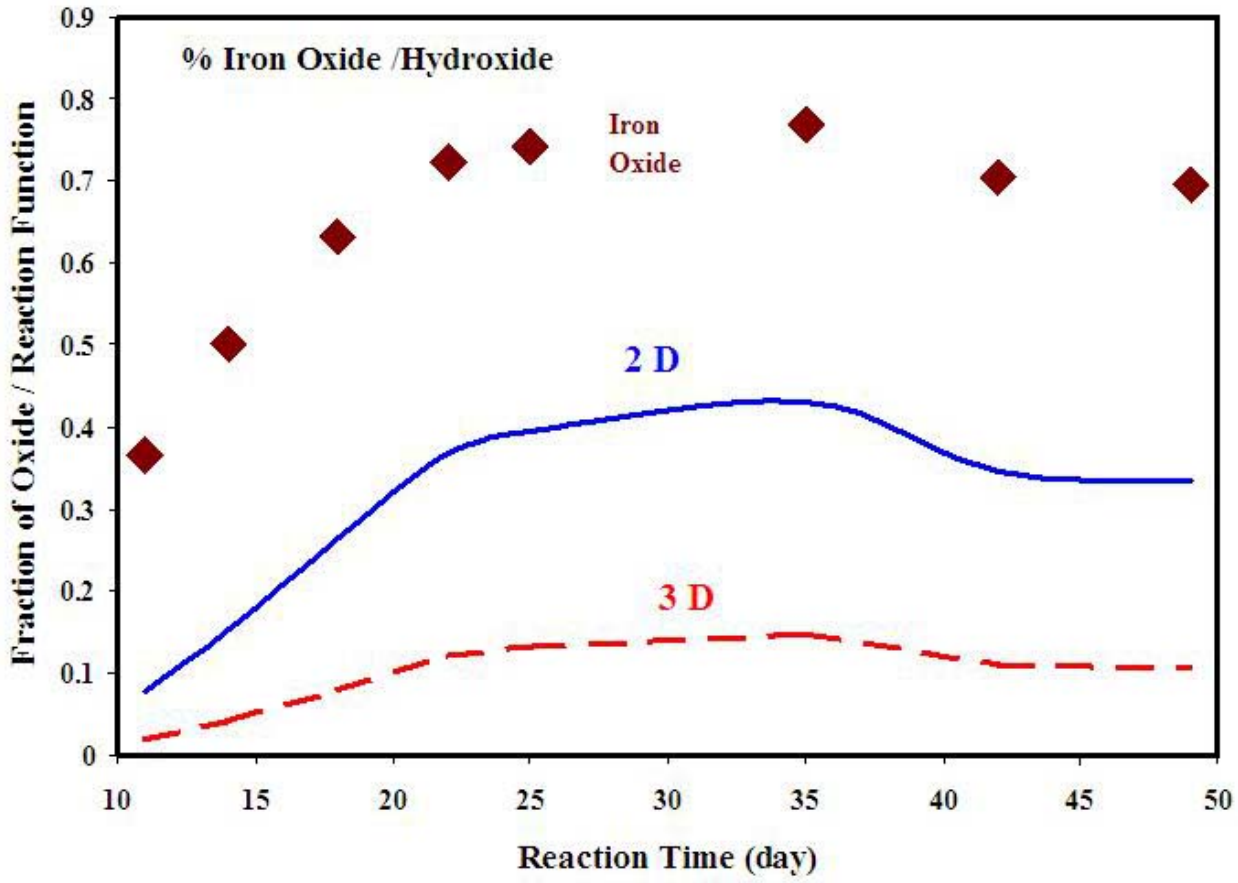

Figure 38. % Iron oxide/hydroxides on the surface of nickel aluminum bronze (NAB) in 10% ammonia and 90% seawater. Symbol represents estimation based on experimental values, 2D and 3D represents the predictions based on 2-dimensional and 3-dimensional diffusion models

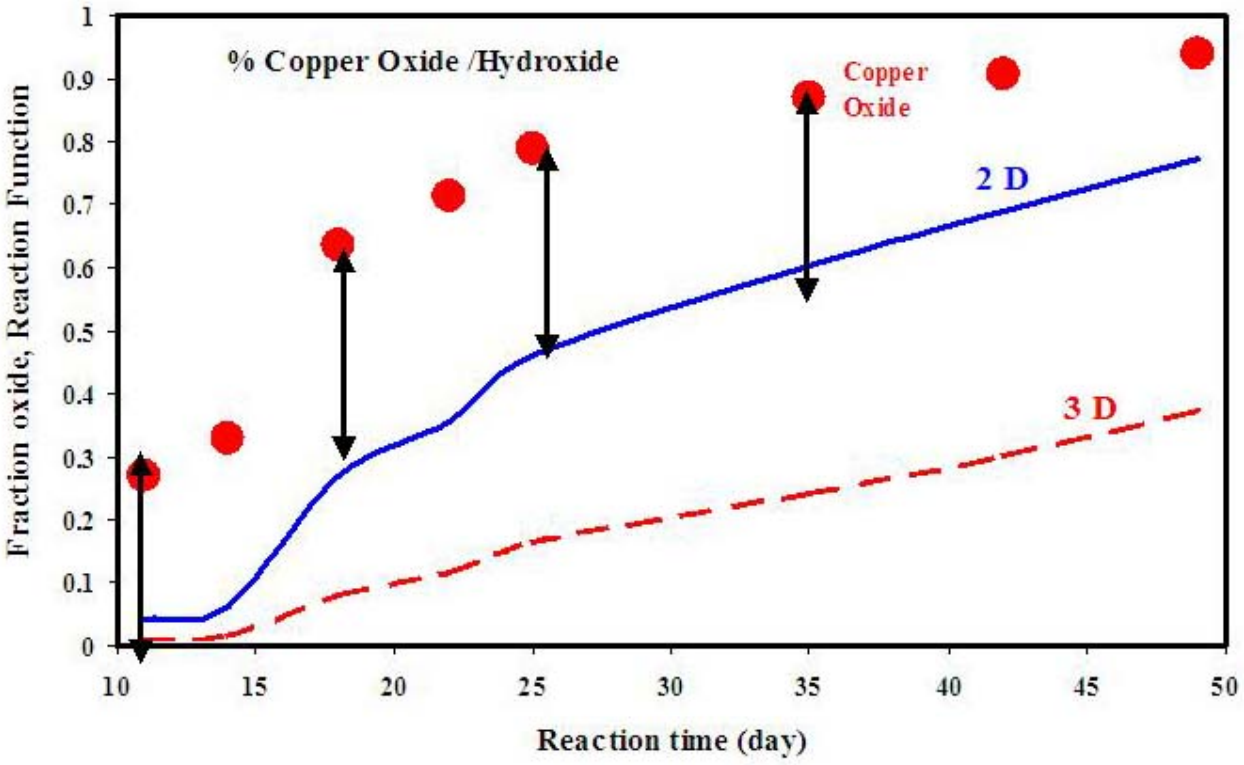

Figure 39. % Copper oxide/hydroxides on the surface of nickel aluminum bronze (NAB) in 10% ammonia and 90% seawater. Symbol represents estimation based on experimental values, 2D and 3D represents the predictions based on 2-dimensional and 3-dimensional diffusion models. Also shown is the constant experimental data shift from 2D model curve

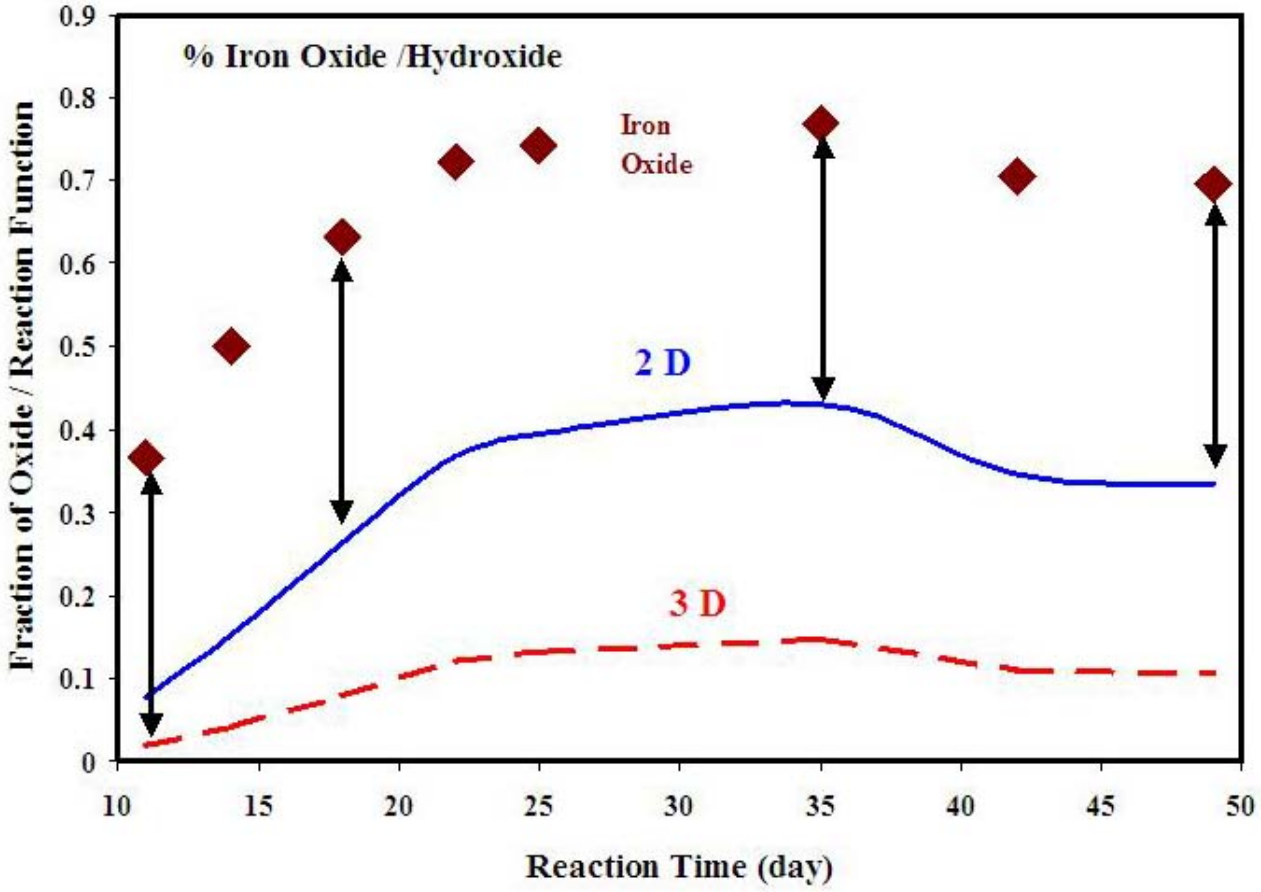

Figure 40. % Iron oxide/hydroxides on the surface of nickel aluminum bronze (NAB) in 10% ammonia and 90% seawater. Symbol represents estimation based on experimental values, 2D and 3D represents the predictions based on 2-dimensional and 3-dimensional diffusion models. Also shown is the constant experimental data shift from 2D model curve

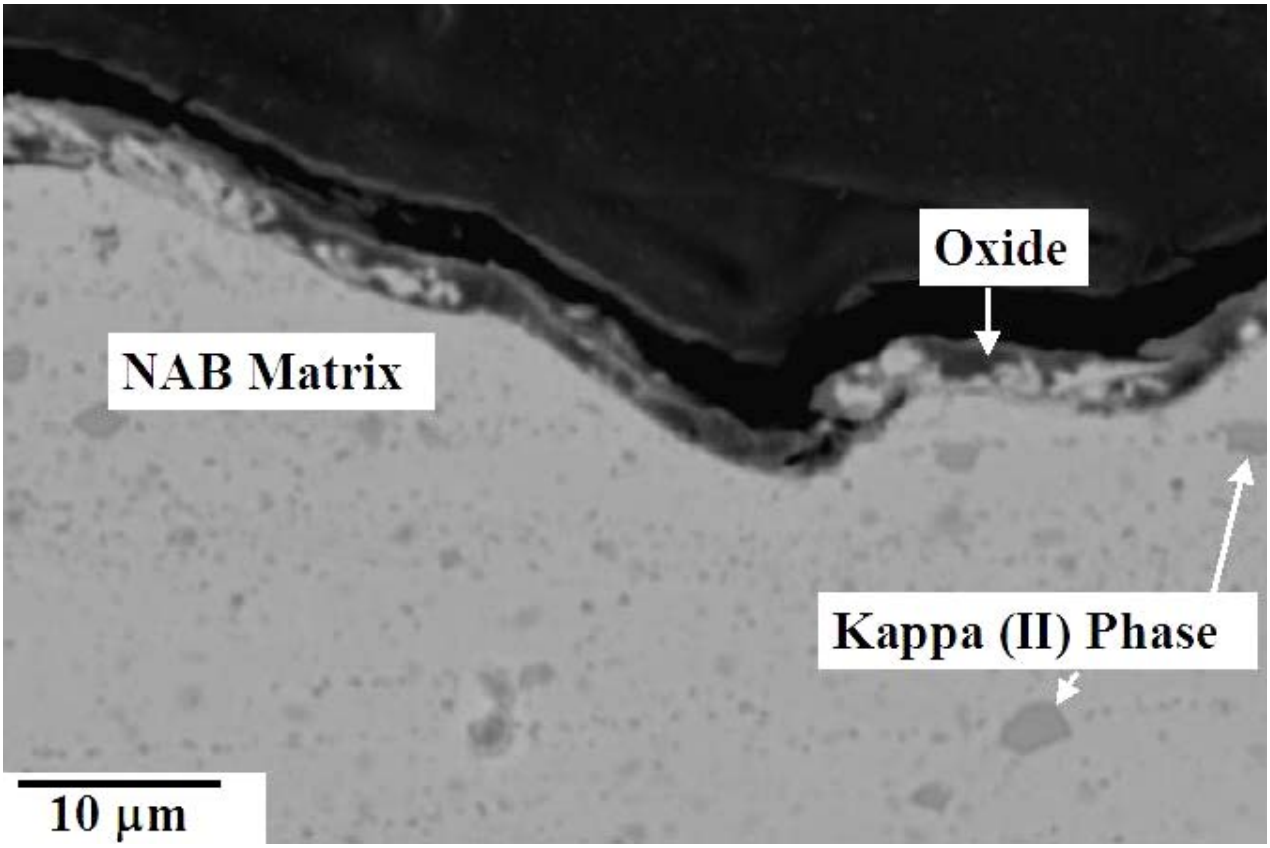

Figure 41. Microstructure of the Cross-sectional view of the polished nickel aluminum bronze (NAB) sample before the corrosion testing in 10% ammonia solution

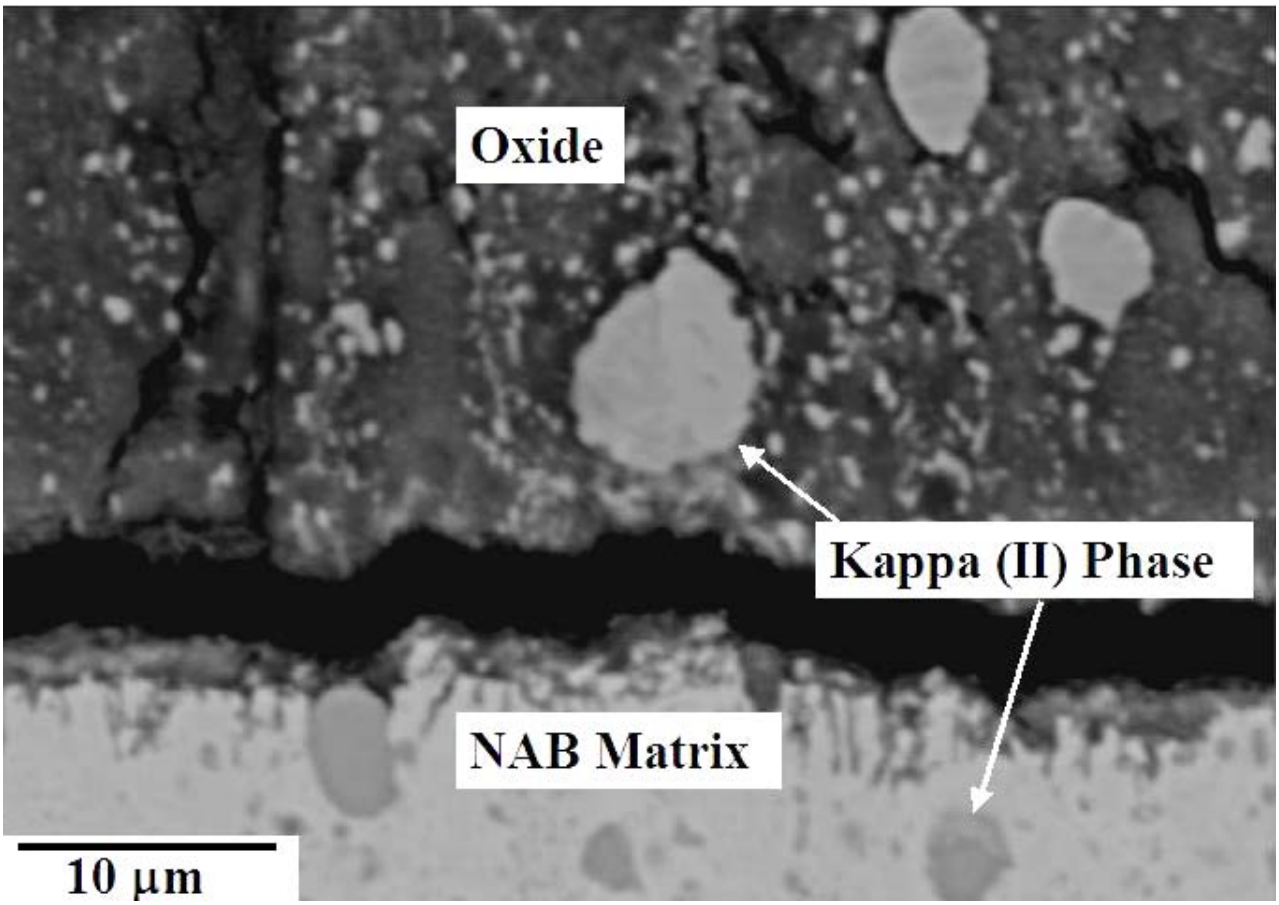

Figure 42 Microstructure of the Cross-section al view of the polished nickel aluminum bronze (NAB) sample after corrosion testing in 10% ammonia solution for 42 days.

Table 1. The rate of oxide formation and the order of the reaction estimated from the weight change measurement for nickel aluminum bronze (NAB) in 10% ammonia and 90% seawater.

Applied External Stress (ksi)	Overall Reaction		Fast Reaction		Slow Reaction	
	Rate (%/day)	Order	Rate (%/day)	Order	Rate (%/day)	Order
0	0.0052	0-0.5	0.0064	0-0.5	0.0029	1.0-2.0
7.5	0.011	0 - 0.5	0.013	0.5	0.0048	2.0
15	0.017	0.5	0.026	0.5	0.0069	2.0

Table 2. The rate of oxide formation and the order of the reaction estimated from the structure change measurement for nickel aluminum bronze (NAB) in 10% ammonia and 90% seawater. No external applied stress

Oxide/ hydroxide	Overall Reaction		Fast Reaction		Slow Reaction		Correction (%)
	Rate (%/day)	Order	Rate (%/day)	Order	Rate (%/day)	Order	
Copper	2.64	0.5	5	0.5	1.5	2	18
Nickel	1.61	0.5	1.85	0.5	1	2	15
Aluminum	1.67	0.5	2.5	0.5	0.69	2.0-2.5	10
Iron	2.22	0.5	3.13	0.5	1	2.5-3.0	50
All oxides/ hydroxides	2.64	0.5	3.2	0.5	0.83	2	29

Table 3. The rate of oxide formation and the order of the reaction estimated from the structure change measurement for nickel aluminum bronze (NAB) in 10% ammonia and 90% seawater. Applied external stress was 7.5 ksi

Oxide/ hydroxide	Overall Reaction		Fast Reaction		Slow Reaction		Correction (%)
	Rate (%/day)	Order	Rate (%/day)	Order	Rate (%/day)	Order	
Copper	2.31	0.5	2.5	0.5	1.25	2	27
Nickel	1.13	0 - 0.5	1.28	0 - 0.5	0.9	2	20
Aluminum	1.56	0.5	2.04	0.5	0.85	2.0-2.5	15
Iron	2.08	0.5	2.63	0.5	0.7	2.5-3.0	56
All oxides/ hydroxides	2.5	0.5	3.13	0.5	1.06	1.5-2.0	29

Table 4. The rate of oxide formation and the order of the reaction estimated from the structure change measurement for nickel aluminum bronze (NAB) in 10% ammonia and 90% seawater. Applied external stress was 15 ksi.

Oxide/ hydroxide	Overall Reaction		Fast Reaction		Slow Reaction		Correction (%)
	Rate (%/day)	Order	Rate (%/day)	Order	Rate (%/day)	Order	
Copper	2.64	0.5	5	0.5	1.5	2	33
Nickel	1.61	0.5	1.85	0.5	1	2	18
Aluminum	1.67	0.5	2.5	0.5	0.69	2.0-2.5	13
Iron	2.22	0.5	3.13	0.5	1	2.5-3.0	66
All oxides/ hydroxides	2.64	0.5	3.2	0.5	0.83	2	40

Distribution

	Copies
DoD - CONUS	
CHIEF OF NAVAL RESEARCH ATTN 332 (A J PEREZ) CORROSION PROGRAM MANAGER 875 N. RANDOLPH STREET ARLINGTON VA 22203-1995	1
COMMANDER NAVAL SEA SYSTEMS COMMAND ATTN SEA 05P24 1333 ISAAC HULL AVE SE STOP 5132 WASHINGTON NAVY YARD DC 20376-5132	1
COMMANDER NAVAL SEA SYSTEMS COMMAND 1333 ISAAC HULL AVE SE STOP 5132 ATTN SEA 05P23 WASHINGTON NAVY YARD DC 20376-5132	1
INTERNAL	
CODE 0115	1
CODE 0112	1
CODE 60	1
CODE 60 (SUDDUTH)	1
CODE 61	1
CODE 612 (RAO)	6
CODE 611	1
CODE 612	1
CODE 612 (FIELDER)	1
CODE 612 (GAIES)	1
CODE 612 (HAYDEN)	1
CODE 612 (PURTSCHER)	1
CODE 612 (ROE)	1
CODE 612 (SUTTON)	1
CODE 612 (SYLVESTER)	1
CODE 612 (WONG)	1
CODE 612 (ZHANG)	1
CODE 612 (BRANDEMARTE)	1
CODE 613	1
CODE 614	1
CODE 615	1
CODE 616	1
CODE 617	1
CODE 63	1
CODE 65	1
CODE 65 (RULE)	1
CODE 66	1
CODE 3442 (TIC-PDF only)	1

This page intentionally left blank

Carderock Division